Sub-Planckian Inflation Due To A Complex Scalar In A Modified Radiative Seesaw Model

Sub-Planckian Inflation Due To A Complex Scalar In A Modified Radiative Seesaw Model

A dissertation submitted in partial fulfillment for the degree of

" Doctor of Philosophy in Science "

Romy Hanang Setya Budhi

1223102011

Supervisor : Prof. Daijiro Suematsu

Graduate School of Natural Science and Technology

Division of Mathematical and Physical Sciences

Kanazawa University

October 2015

Dedicated to:
Allah My Lord
the All-beneficent, the All-merciful

Indeed, in the creation of the heavens and the earth
and the alternation of night and day
are signs for those of understanding.
(Ali 'Imran: 190)

List of publications:

1. **Romy H. S. Budhi**, Shoichi Kashiwase and Daijiro Suematsu, *Inflation in a modified radiative seesaw model*, Phys. Rev D 90, 113013 (2014).

KANAZAWA UNIVERSITY

Abstract

Graduate School of Natural Science and Technology
Division of Mathematical and Physical Sciences

Doctor of Science

by Romy Hanang Setya Budhi

Recent CMB observation seems to strongly support the existence of inflation. Even so, only a few realistic inflation scenarios which have close relation to particle physics seems to have been known unfortunately. Including the inflation, there are several issues beyond the Standard Model of particle that have been clarified by observations: neutrino mass and mixing, existence of dark matter and baryon asymmetry that need to be explained in a comprehensive way. The radiative neutrino mass generation with an inert doublet is known as a promising model that successfully explains those three phenomenology issues employed at a TeV scale. Therefore, here we consider an extension of the radiative neutrino mass model by using a complex singlet scalar to explain inflation phenomena as well. The feature of the radiative neutrino mass model can be kept as long as the new scalar singlet is much heavy compared to the right-handed neutrino and the inert doublet.

To evade the Lyth bound, a minimum requirement to generate sufficient tensor-to-scalar ratio constrained by recent observation, a particular scalar potential form is chosen such that the inflaton is restricted to evolve along a spiral-like valley and it behaves as single field inflaton. As a result of long trajectory taken during inflation, the inflaton can be kept to be a sub-Planckian field. It is shown that the feature of the inflaton is similar to the power-law chaotic inflation but having better prediction.

Acknowledgements

First of all, I would like to express my gratitude to Prof. Daijiro Suematsu, my kind supervisor, who supports me in many ways. Thank you very much for your guidance and dedication during the research and completing the dissertation. I would like to give my respect to Prof. Ken-Ichi Aoki, Prof. Jisuke Kubo, Prof. Mayumi Aoki, and Prof. Daisuke Yonetoku for their comments and discussion. I also would like to thank the staffs and the students of Institute for Theoretical physics Kanazawa University for their hospitality and friendship.

I am thankful to the Directorate General of Higher Education (DIKTI), Indonesia, and Kanazawa University, Japan, for financial support through the Joint Scholarship Program.

The last but not least, deeply from my heart, I would like to thank my parents (Rokidi-Mudjidah), my parent in law (Arief Hermanto-Sri Rahayuningsih) and my wife (Annisa Fitria) for their unconditional love and encouragement through all of my days.

Contents

List of Figures

List of Tables

Chapter 1

Introduction

1.1 Background and purposes

The standard model (SM) of particle is now considered to be extended due to unsuccessful explanation of some observational phenomena in this framework. Those phenomena are the neutrino masses and mixing [1–4], the existence of dark matter [5, 6] and the baryon number asymmetry in the universe [7, 8]. Finding a model that can explain all those phenomena simultaneously without causing any tension to other phenomenological problems would be a crucial step to understand the new physics beyond the SM. One of a promising candidate for that purpose is a simple extension of the SM with an additional doublet scalar and three right-handed neutrinos. Z_2 symmetry is also imposed as a new one. The new particles are signed Z_2-odd parity meanwhile all of the SM particles are signed Z_2-even parity. Since the additional doublet scalar is assumed to have no vacuum expectation value and than it is forbidden to interact with the SM fermions due to this exact Z_2 symmetry, it is named an inert double [9]. Naturally, this model provides a mechanism to generate small neutrino masses at one-loop level and also dark matter candidate which could be the lightest Z_2-odd particle. Moreover, there are a hint to produce baryon number asymmetry through spharelons of electroweak vacuum transition from lepton number asymmetry produced from the decay of the right-handed neutrinos [10]. Several studies [11–13] show a simultaneous explanation of those three

phenomenology beyond the SM can be achieved under minimal tensions with other phenomenology such as lepton flavor violating processes. In fact, it is found to be successfully realized if the dark matter candidate is the lightest neutral component of the inert doublet with mass $\mathcal{O}(1)$ TeV. The baryon number asymmetry can also be successfully explained through resonant leptogenesis due to the mass degeneracy of right-handed neutrinos with mass of order TeV scale.

On the other hand, the existence of inflationary expansion of the universe at very early time is strongly supported by the CMB observation. Severe observational constraints such as Planck 2013 and Bicep2 restrict the allowed inflation model now [14, 15]. They completely disfavor any model predicting at almost scale invariant and blue tilted scalar power spectrum. They also prefer to a single field model over more complicated scenarios. There are also theoretical constraints such as the Lyth bound [16] that restricts the allowed field value to realize the sufficient tensor-to-scalar ratio. The η problem is another one that is a kind of hierarchy problem between the inflaton mass and the Hubble parameter. In single field inflation models, since the Lyth bound prevents the inflaton field to have a value below Planck scale, the higher order terms suppressed by the Planck mass appear to ruin the flatness of the inflaton potential. If there is no symmetry protecting the potential, this difficulty is caused and the η problem is inevitable as well. The observation by Planck 2015 [17] tightening the tensor-to-scalar ratio constraint to be $r_{0.002} < 0.11$ (95 % CL) so that only a few model can still survive, as instances the hiltop quartic model, R^2-inflation, Higgs-inflation and power-law chaotic inflation with power less than two.

From such many inflation models that survive from the observational constraints, there are not so many inflaton candidates that play any role in particle physics. Even so, they have still problems. As instances, the power law chaotic inflation which is motivated by axion monodromy suffers trans-Planckian problem due to the Lyth bound and the η problem, and the Higgs inflation suffers from the unitary problem caused by a large non-minimally coupling [18, 19].

Motivated by the above facts, we consider an extension of the radiative seesaw model with a complex scalar to explain the inflation of the universe as well without disturbing favorable features of the original model. To evade the Lyth bound and

the η problem, the field value of the inflaton which corresponds to the complex scalar will be kept in sub-Planckian values by choosing a potential in such a way that only a particular dynamics of the inflaton is allowed. In this scenario, the spectral index and the tensor-to-scalar ratio could have values in a region favorable by the recent CMB observations depending on the parameter sets in the inflaton potential.

1.2 Outline of the thesis

This dissertation will consist of five chapters. In chapter 1, the motivational background and the purposes are mentioned. In chapter 2, we explain the concept of the inflation idea in the early time of the universe, including how the inflation criteria is manifested in the several realizations, the cosmological perturbations from inflation which are seeds of inhomogeneity of the energy density that eventually grow to be any structure in the universe seen today, and in the last part of the chapter we explain theoretical constraints on the inflation models, the Lyth bound and the η problem. In chapter 3, the radiative neutrino masses model and its extension due to an additional complex scalar are elaborated. Then in chapter 4, the scenario of inflation due to the complex scalar in the modified radiative neutrino mass model is explained. The calculation and also the predictions favored by the recent CMB observations are also clarified in this part. Finally, in chapter 5 the results and discussion are summarized.

Chapter 2

Physics of Inflation

2.1 Standard Big Bang cosmology and its problems

The Big Bang cosmology is known to be a successful model describing the evolution of the universe. The Big Bang cosmology assumes that the universe originates from an infinitely hot and dense gaseous state and expands being cooled down afterward. This theory is extremely successful to explain fundamental cosmological observations: the homogenous cosmic expansion, the cosmic microwave background radiation (CMB) and the abundance of light elements [20]. However, the behavior of the early universe before nucleosynthesis is uncertain. The problems related to the initial condition of the universe such as the horizon problem, the flatness problem, the initial singularity problem and so on, are motivations to introduce the hypothesis of inflation, that is there was a period of very rapid expansion of the universe at very early times [21–23].

The Big Bang theory is based on the cosmological principle stating that the universe is homogenous and isotropic on the largest scales and physical laws governed by general relativity. The only possible geometry of the universe obeying

the symmetry dictated by the cosmological principle is the Friedmann-Robertson-Walker (FRW) spacetime with a metric defined as

$$ds^2 = -dt^2 + a^2(t)\left[\frac{dr^2}{1-\kappa r^2} + r^2(d\theta^2 + \sin^2\theta d\phi^2)\right], \tag{2.1}$$

which is completely determined by cosmic scale factor $a(t)$, and the curvature of spatial hypersurface κ at a constant cosmic time t. Here, $\kappa = -1, 0, +1$ describe open universe, flat universe and closed universe, respectively. The scale factor $a(t)$ represents the radius of the universe at a given time. It is sometimes more convenient to adopt comoving coordinate x^i, for which the FRW metric can be represented as $ds^2 = -dt^2 + a^2(t)\gamma_{ij}dx^i dx^j$. The information of spatial curvature of the hypersurface is contained in the spatial metric γ_{ij}. Here, the length L between two points in the comoving surface is constant all the time, but the physical length grows as the universe expands $a(t)L$. The cosmological principle also requires that the gaseous of the universe behave as a perfect fluid with the stress energy tensor given by

$$T_{\mu\nu} = (\rho + p)U_\mu U_\nu - p g_{\mu\nu}. \tag{2.2}$$

where ρ and p denote the energy density and the pressure of the fluid, respectively. Inserting the FRW metric to the Einstein field equation $R_{\mu\nu} - \frac{1}{2}\mathcal{R}g_{\mu\nu} = 8\pi G T_{\mu\nu}$, the-00 and the-$ij$ components of the Einstein equation lead to the Friedmann equations

$$H^2 = \frac{\rho}{3M_{pl}^2} - \frac{\kappa}{a^2}, \tag{2.3}$$

$$\frac{\ddot{a}}{a} = -\frac{1}{6M_{\rm pl}}(\rho + 3p), \tag{2.4}$$

where $M_{\rm pl} := \frac{1}{\sqrt{8\pi G}} = 2.435 \times 10^{18}$ GeV is the reduced planck mass and $H := \frac{\dot{a}}{a}$ is called the Hubble parameter, which is estimated today as $H_0 = (67.3 \pm 1.2)$ km s^{-1} Mpc^{-1} [24]. The conservation of energy-momentum implies the continuity equation

$$\dot{\rho} + 3H(\rho + p) = 0. \tag{2.5}$$

From this continuity equation, the behavior of the energy density can be derived

during the expansion of the universe as follows: $\rho \propto a^{-3}$ for matter for which the pressure is negligible compared to the energy density, and $\rho \propto a^{-4}$ and $p = \rho/3$ for radiation. The relation $p = -\rho$ is satisfied for domination of the cosmological constant in the Einstein equation. Thus, its energy density is kept constant throughout the expansion.

The first puzzle of the standard theory of cosmology is related to homogeneity and isotropy of the universe. The observations of the CMB show that widely separated regions of the space have almost the same temperature about 2.728° K with temperature variations of the order 10^{-5} [25]. This is remarkable since those regions appear to be causally disconnected at the recombination time when radiation is decoupled from matter and the CMB was emitted. On the other hand, the universe must be homogenous enough at this decoupling time to explain the homogeneity of the CMB observed today. Thus, it is difficult to understand how those regions share physical properties if they have never causally interacted each other. This puzzle is known as the *horizon problem*. There is also a relevant question how structures we know today such as stars and galaxies have formed from such highly homogenous early universe. Conceptually, two points are said to be causally connected if there is a null geodesic of the photon between them, $ds^2 = 0$. Taking account of only the radial direction and defining conformal time $\tau := \int dt/a(t)$ from the FRW metric $ds^2 = -dt^2 + a^2(t)d\chi^2 := a^2(\tau)\left[-d\tau^2 + d\chi^2\right]$, the null geodesic is given by $\Delta\chi = \pm\Delta\tau$. If the Big Bang is considered to start from $t_i = 0$, the observable of greatest comoving distance at time t is

$$\chi_{\rm ph}(\tau) = \int_{t_i}^{t} \frac{dt}{a} = \int_{a_i}^{a} (aH)^{-1} d\ln a. \tag{2.6}$$

The quantity $\chi_{\rm ph}(\tau)$ is called (comoving) *particle horizon*, meanwhile $(aH)^{-1}$ is called comoving *Hubble radius*. If the pressure and the energy density of the fluid dominating the universe satisfy the equation of state $p := w\rho$ (i,e $w = 0$ for matter dominated universe, $w = 1/3$ for radiation dominated universe, and $w = -1$ for vacuum energy domination), one can derive behavior of the Hubble radius as $(aH)^{-1} = \dot{a}^{-1} = \beta a^{\frac{1}{2}(1+3w)}$ by using Friedmann equation. Here, β is a constant.

Therefore, the comoving Hubble horizon is found for $w > -1/3$

$$\chi_{\rm ph}(t) = \frac{2\beta}{1+3w} a(t)^{\frac{1}{2}(1+3w)} = \frac{2}{1+3w}(aH)^{-1}. \tag{2.7}$$

This shows that the particle horizon could be almost equal to the Hubble radius in all epochs of the Big Bang history. Particles separated more than the particle horizon could have never communicated each other and completely disconnected causally. However, although particles separated more than the Hubble radius cannot communicate now, there is a possibility that they were in the causal contact early on. The present Hubble radius could be much larger than those at the CMB time. By comparing them, it can be shown that there were about 10^{-6} of causally disconnected regions in the present horizon [26].

The next puzzle comes from the first Friedmann equation which implies

$$\Omega(t) - 1 = \frac{\kappa}{(aH)^2}, \quad \Omega(t) := \frac{\rho(t)}{\rho_{\rm cr}(t)}, \quad \rho_{\rm cr}(t) := \frac{3H^2}{8\pi G}. \tag{2.8}$$

The present density parameter $\Omega(t_0)$ is measured 1.02 ± 0.02 with the best-fit age of universe t_0 is 13.7 ± 0.2 Gyr $\simeq 4.3 \times 10^{17}$ s [27]. The scale factor evolves like $a \sim t^p$ with $p < 1$. Therefore, the factor $(aH)^{-2} = \dot{a}^{-2}$ grows with time. If we go back in time, $|\Omega - 1|$ would be closer to zero to explain the present value of density parameter. For example, the assumption that the universe is dominated by matter from the recombination time $t_r \simeq 1.2 \times 10^{13}$ s to the present day requires $|\Omega(t_r) - 1| < 10^{-4}$. Furthermore, assuming that the universe is dominated by radiation from Planck time $t_{\rm pl} \simeq 10^{-43}$ s to the time of matter-radiation equality $t_{\rm eq} \simeq 2.0 \times 10^{12}$ s, the density parameter at Planck time should satisfy $|\Omega(t_{\rm pl}) - 1| < 10^{-64}$. This value shows that if the initial energy density $\rho(t_{\rm pl})$ is chosen to be smaller than the critical energy density $\rho_{\rm cr}(t_{\rm pl})$ by $\rho_{\rm cr}(t_{\rm pl}) \times 10^{-64}$, the universe would expand quickly before structures are formed in it. On the other hand, taking the initial energy density larger would make it collapses too fast. This extreme fine-tuning, called *flatness problem*, demands more natural way to explain it.

The main point of the horizon problem is how to make the causally disconnected regions detected in the CMB could communicate in the past. Thus, if the Hubble radius was larger in the past $(a_I H_I)^{-1}$ compared to the present Hubble

radius $(a_0H_0)^{-1}$, the horizon problem can be solved. The period during shrinking of the Hubble radius is called inflation period. This shrinking Hubble radius during inflation should be followed by the growing Hubble radius afterwards. This gives the following picture. We consider two particles separated by the distance $\lambda < (aH)^{-1}$. They communicate during inflation until at a moment before horizon exit $\lambda = (aH)^{-1}$. Their physical properties are freezed during $\lambda > (aH)^{-1}$ afterwards until horizon reentry after the inflation is terminated. After that, the particles follow ordinary Big Bang cosmology. Assume that the universe is dominated by radiation from a energy scale near the GUT scale $T_E \simeq 10^{14}$ GeV up to today, the comparison of both Hubble radius gives $a_0H_0/a_EH_E = a_E/a_0 \simeq T_0/T_E \simeq 10^{-27}$ thus $(a_IH_I)^{-1} > 10^{27}(a_EH_E)^{-1}$. $T_0 \simeq 10^{-3}$ eV is the recent CMB temperature and $a \sim T^{-1}$ is obtained from the entropy conservation. By adding an assumption that the Hubble parameter is approximately constant during the inflation, the universe should expand exponentially by factor a $\ln(a_E/a_I) > 62$ to solve the above mentioned flatness problem. Later, this factor is called e-folding number of inflation.

The shrinking Hubble radius as the inflation criteria is equivalent to some other criteria [28, 29]:

- Since $d(aH)^{-1}/dt = -\ddot{a}/(\dot{a}^2)$ is satisfied, accelerated expansion $\ddot{a} > 0$ is required.
- Since $\frac{d(aH)^{-1}}{dt} = -\frac{1}{a}(1-\varepsilon)$ where $\varepsilon := -\frac{\dot{H}}{H^2}$ is satisfied, the shrinking Hubble radius implies $\varepsilon < 1$. Furthermore, if *e-folding number* N is defined through $dN := d\ln a = Hdt$, $\varepsilon = -\frac{d\ln H}{dN} < 1$ means that fractional change of Hubble parameter per e-folding should be kept small during the inflation. To realize the smallness of ε, its fractional change should be also small $|\eta| := \left|\frac{d\ln\varepsilon}{dN}\right| = \left|\frac{\dot{\varepsilon}}{H\varepsilon}\right| < 1$. Thus, the shrinking condition of the Hubble radius is equivalently stated as condition $\varepsilon, |\eta| < 1$.
- Using Friedmann equations, the parameter ε can be written as $\varepsilon = \frac{3}{2}(1+w)$ for the fluid satisfies $p = w\rho$. Thus, as $\varepsilon < 1$ during inflation, this can be realized by the negative pressure $w < -1/3$.

2.2 Realization of inflation

It is well known that the Einstein equation of gravity $R_{\mu\nu} - \frac{1}{2}\mathcal{R}g_{\mu\nu} = 8\pi G T_{\mu\nu} + \Lambda g_{\mu\nu}$ can be derived directly from an action principle: The action is stationary under small variations of the metric tensor. The action leading to the Einstein equation can be written as a composition between a gravitational action, known as Hilbert-Einstein action S_{EH} and a matter action S_M. The action is $S = S_{EH} + S_M$ where

$$S_{EH} = -\int d^4x\sqrt{-g}\frac{M_{\rm pl}^2}{2}\left(\mathcal{R} + 2\Lambda\right), \tag{2.9}$$

$$S_M = \sum_{\rm fields}\int d^4x\sqrt{-g}\mathcal{L}_{\rm fields}, \tag{2.10}$$

here $g := \det(g_{\mu\nu})$, $M_{\rm pl}$ is the reduced Planck mass and $\mathcal{R}$ is the Ricci scalar [30]. The variation of S_{EH} and S_M are given as

$$\delta S_{EH} = \frac{M_{\rm pl}^2}{2}\int d^4x\sqrt{-g}\left(R^{\mu\nu} - \frac{1}{2}\mathcal{R}g^{\mu\nu} - \Lambda g^{\mu\nu}\right)\delta g^{\mu\nu}, \tag{2.11}$$

$$\delta S_M = -\frac{1}{2}\sum_{\rm fields}\int d^4x\sqrt{-g}T^{\mu\nu}_{\rm fields}\delta g^{\mu\nu}, \tag{2.12}$$

so that the variation principle $\delta S/\delta g_{\mu\nu} = 0$ leads to the Einstein equation of gravity. Through this action, we will show later how inflation criteria $\varepsilon = -\dot{H}/H^2 < 1$ could be realized by some action form.

2.2.1 Slow-roll inflation

Lets consider a scalar field ϕ which is minimally coupled[1] to Einstein gravity through its action

$$S_M = \int d^4x\sqrt{-g}\mathcal{L} = \int d^4x\sqrt{-g}(X - V(\phi)), \tag{2.13}$$

[1]Minimal coupling refers to the case with the coefficient $\xi = 0$ in the interaction term $\frac{1}{2}\xi\mathcal{R}\phi^2$ in the Lagrangian density. Otherwise, it's called non-minimally coupled scalar to gravity.

where $X := -\frac{1}{2}g^{\mu\nu}\partial_\mu\phi\partial_\nu\phi$ is canonical kinetic term and $V(\phi)$ denotes potential term of the scalar field ϕ. If the signature of the metric is taken as $(-,+,+,+)$, the variation of this action respected to the metric tensor leads to the energy-momentum tensor given by

$$T_{\mu\nu} = -\frac{2}{\sqrt{-g}}\frac{\delta S}{\delta g^{\mu\nu}} = \mathcal{L}g_{\mu\nu} + \partial_\mu\phi\partial_\nu\phi. \tag{2.14}$$

If the scalar field ϕ is spatially homogenous in the FRW spacetimes, $T^{\mu\nu}$ takes the form of perfect fluid and its energy density and pressure can be written as

$$\rho = \frac{\dot{\phi}^2}{2} + V(\phi), \quad p = \frac{\dot{\phi}^2}{2} - V(\phi), \tag{2.15}$$

respectively. Hence, as one of the inflation condition is when $\rho + 3p < 0$ should be satisfied, an acceleration expansion can be realized if the potential term dominates $V(\phi) > \dot{\phi}^2/2$. This realization of the exponential expansion of the universe is known as a standard mechanism to generate inflation. It is called slow-roll approximation [20].

Substitution of energy density of the scalar field in to time derivative of the Friedmann equation $H^2 = \rho/(3M_{\rm pl}^2)$ gives

$$2H\dot{H} = \frac{1}{3M_{\rm pl}^2}\left[\dot{\phi}\ddot{\phi} + V'\dot{\phi}\right], \tag{2.16}$$

where we denote $V' := dV/d\phi$. On the other hand, the second Friedmann equation leads to an identity $\dot{H} + H^2 = -\frac{1}{6M_{\rm pl}^2}(\rho + 3p)$. Therefore, $\dot{H} = -\frac{1}{2M_{\rm pl}^2}(\rho + p) = -\frac{1}{2M_{\rm pl}^2}\dot{\phi}^2$. Substitution of $\dot{H}$ to the equation (2.16) leads to the equation of motion

$$\ddot{\phi} + 3H\dot{\phi} + V' = 0. \tag{2.17}$$

This semiclassical equation of motion, where quantum fluctuations of the field are considered small enough, might be understood as that in classical mechanics for a ball rolling down with friction in the potential V. The friction term $3H\dot{\phi}$ arises due to the expansion of the universe which causes the red shifting of the field momentum during expansion. Additional friction terms might be included here, such us $\Gamma\dot{\phi}$ to

represent decay of the field causing inflation, the inflaton ϕ, to other particles with decay rate Γ^{-1}.

Domination of the potential term in the energy density should be kept long enough to generate inflation sufficiently. Therefore, the potential would be almost flat during inflation since the kinetic energy term is kept small enough. Furthermore, acceleration of the field has to be very small as the kinetic energy is negligible during that time. Thus, the equation of motion of the field and the Hubble scale can approximately given to be

$$3H\dot{\phi} \simeq -V', \tag{2.18}$$

$$H^2 \simeq \frac{V}{3M_{\rm pl}^2}, \tag{2.19}$$

respectively. The equation (2.19) tells us how the cosmic scale factor grows by factor $a(t) = a_1 \exp H(t - t_1) := a_1 \exp N$, $a(t_1) := a_1$ during inflation. The number of e-folds of the growth in the scale factor when ϕ rolls from ϕ_1 to ϕ_2 is

$$N(\phi_1 \to \phi_2) = \int_{t_1}^{t_2} H dt \simeq \int_{\phi_1}^{\phi_2} \frac{H}{\dot{\phi}} d\phi \simeq 3 \int_{\phi_1}^{\phi_2} \frac{H^2}{-V'} d\phi \tag{2.20}$$

$$\simeq -\frac{1}{M_{\rm pl}^2} \int_{\phi_1}^{\phi_2} \left(\frac{V}{V'} \right) d\phi. \tag{2.21}$$

To solve the flatness problem, the e-folding number is required to have a value about $50 - 60$. This number depends on the processes after horizon exits such as reheating phenomena and others [31, 32]. Slowly-varying Hubble parameter $\{\varepsilon, \eta\}$ could be guarantied by imposing the following conditions:

$$\varepsilon = -\frac{\dot{H}}{H^2} = \frac{\dot{\phi}^2/2}{M_{\rm pl}^2 H^2} \simeq \frac{M_{\rm pl}^2}{2} \left(\frac{V'}{V} \right)^2 := \varepsilon_V \ll 1, \tag{2.22}$$

$$\delta := -\frac{\ddot{\phi}}{H\dot{\phi}} \ll 1, \tag{2.23}$$

$$\eta = 2(\varepsilon - \delta) \ll 1, \tag{2.24}$$

$$\eta_V := \delta + \varepsilon \simeq M_{\rm pl}^2 \frac{V''}{V} \ll 1. \tag{2.25}$$

These ε_V and η_V are called slow-roll parameters which is simply written as ε and η respectively except there is urgency to differentiate the notation.

2.2.2 Kinetically driven inflation

The slow-roll approximation strongly restricts the shape of the potential $V(\phi)$ because of $\varepsilon_V \ll 1$. The potential should be flat enough in some interval in order to realize sufficient inflation. In contrast, the Hubble slow-roll conditions, $\{\varepsilon, |\eta|\} < 1$ allow to relax the constraint. The condition $\dot{H} < H^2$ can be possibly caused not by potential domination but by the kinetic energy domination which is allowed by non-trivial dynamics. A possible scenario of this type of inflation is given by considering a non-canonical kinetic term in the gravitational action [33, 34], such as

$$S = \int d^4x\sqrt{-g}\left(\frac{M_{\rm pl}^2}{2}\mathcal{R} + P(\varphi, X)\right). \tag{2.26}$$

The energy-momentum tensor of this action is

$$T_{\mu\nu} = P(\varphi, X)g_{\mu\nu} + \frac{\partial P(\varphi, X)}{\partial X}\partial_\mu\varphi\partial_\nu\varphi. \tag{2.27}$$

This equation shows that if $\partial_\mu\varphi$ is a time-like vector (i.e $X > 0$), the normalization of $u_\mu := \partial_\mu\varphi/(\sqrt{2}X)$ leads to energy-momentum tensor

$$T_{\mu\nu} = (\rho + p)u_\mu u_\nu + P(\varphi, X)g_{\mu\nu}, \tag{2.28}$$

$$\rho = 2XP_{,X} - P, \quad p = P(\varphi, X), \tag{2.29}$$

where $P_{,X} := \frac{\partial P(\varphi,X)}{\partial X}$. Hence, the accelerated expansion can be realized even without potential domination in the Lagrangian density, as long as condition $XP_{,X} < P$ is satisfied, i.e. either (i) when X is small that corresponds to slow-roll inflation driven by field potential, or (ii) $P_{,X}$ is small. This type of inflationary model is called k-inflation [33–38]. Taking flat Friedmann universe as the background, then two independent equations for two unknown background variables $\phi(t)$ and time

dependent cosmic scale-factor $a(t)$ can be written down in the form

$$H^2 = \frac{\rho}{3M_{\rm pl}^2}, \quad \dot{\rho} = -3H(\rho + p). \tag{2.30}$$

Therefore, to describe expanding universe, that is for $H > 0$, ones should solve field evolution given from time derivative of H^2. In case of $X = \frac{1}{2}\dot{\varphi}^2$ as an example, the field dynamics equation is given by

$$\left(\ddot{\varphi} + 3H\dot{\varphi}\right) P_{,X} + 2X\ddot{\varphi}P_{,XX} + 2XP_{,X\varphi} - P_{\varphi} = 0. \tag{2.31}$$

2.2.3 Modified gravity inflation

Two previous inflation realizations are based on an assumption that the gravitation action takes the form of Hilbert-Einstein action (2.9), and where we consider the fields that generate the inflation as additional ingredient in the spacetimes. However, even without a matter field content, inflation can be realized as long as the gravitational action sector is allowed to be modified. Writing the action as

$$S = \int d^4x\sqrt{-g}\left(\frac{M_{\rm pl}^2 f(R)}{2} + \mathcal{L}_{\rm matter}\right), \tag{2.32}$$

the variation of this action with respect to the metric leads to a field equation

$$F(R)R_{\mu\nu} - \frac{1}{2}f(R)g_{\mu\nu} - \nabla_\mu\nabla_\nu F(R) + g_{\mu\nu}\Box F(R) = \frac{1}{M_{\rm pl}^2}T_{\mu\nu} \tag{2.33}$$

where $\Box := g^{\mu\nu}\nabla_\mu\nabla_\nu$ is the covariant d'Alembertian operator associates to the covariant derivative ∇_μ, $T_{\mu\nu}$ is the energy-momentum tensor of the matter field and $F(R) := df(R)/dR$ for a Ricci scalar R of the Ricci tensor $R_{\mu\nu}$.

The Ricci tensor and the Ricci scalar completely depend on the metric $g_{\mu\nu}$. Thus, in the FRW universe, they can be written in term of the Hubble parameter. The components of the Ricci tensor are found to be $R_{00} = 3(\dot{H} + 62H)$ and $R_{ij} = 3(\dot{H} + 3H^2 + (2\kappa/a^2))g_{\mu\nu}$ meanwhile the Ricci scalar is $R = 6(\dot{H} + 2H + (\kappa/a^2))$. In case of a perfect fluid in the flat FRW background, the field equation (2.33) turns

to be Friedmann-like equations as follows [39–44] :

$$3FH^2 = \frac{(FR - f)}{2} - 3H\dot{F} + \frac{\rho}{M_{\rm pl}^2}, \tag{2.34}$$

$$-2F\dot{H} = \ddot{F} - H\dot{F} + \frac{\rho + p}{M_{\rm pl}^2}, \tag{2.35}$$

where ρ and p are the energy density and the pressure of the fluid, respectively. The continuity equation

$$\dot{\rho} + 3H(\rho + p) = 0 \tag{2.36}$$

is also hold as a consequence of the energy-momentum conservation $\nabla_\mu T^\mu_\nu = 0$.

To associate with the inflation of the universe, lets assume that the $f(R)$ is explicitly written in the form $f(R) = R + \alpha R^2, (\alpha > 0, n > 0)$. When the matter is absent ($\rho = 0$), the first Friedman-like equation (2.34) gives

$$3(1 + n\alpha R^{n-1})H^2 = \frac{1}{2}(n-1)\alpha R^2 - 3n(n-1)\alpha H R^{n-2}\dot{R}, \tag{2.37}$$

which is under an assumption $(1 + n\alpha R^{n-1}) \simeq n\alpha R^{n-1}$, it gives

$$H^2 \simeq \frac{n-1}{6n}\left(R - 6nH\frac{\dot{R}}{R}\right). \tag{2.38}$$

Thus, the inflation condition $\varepsilon < 1$ can be satisfied for $\varepsilon = -\frac{\dot{H}}{H^2} \simeq \frac{2-n}{(n-1)(2n-1)}$ if we take $n > (1 + \sqrt{3})/2$ [43]. One of the inflation model favorable by the recent observation based on this kind of the inflation realization is the Starobinsky model in which it defines $f(R) := R + \frac{R^2}{6M_{\rm pl}^2}$ [45].

2.3 Cosmological Perturbation and Inflation

Cosmological perturbation is a cornerstone of modern cosmology to describe the formation of structures of the universe and its evolution. During inflation stage, seeds of inhomogeneities of the universe are produced by quantum fluctuation and

eventually grow to classical density perturbation due to a rapid expansion. As energy density is dominated by the inflaton field during inflation stage, perturbation of the energy density or of the energy-momentum tensor induces inflaton perturbation and vice versa. On the other hand, perturbation of the energy-momentum tensor induces the perturbation of the metric as well, through Einstein's field equation. It shows how the perturbations of the inflaton and of the metric field are closely related each other and could not be investigated separately.

The inflaton field could be divided into homogenous classical component $\varphi(t)$ and quantum fluctuation which depends on hypersurface coordinate $\delta\varphi(t,x)$ such that $\varphi(t,x) = \varphi(t) + \delta\varphi(t,x)$. Inflaton fluctuations imply local densities fluctuation $\delta\rho(x)$ which is preserved after inflation. Local fluctuations in the CMB temperature $\Delta T(x)$ which is proportional to $\delta\rho(x)$ are therefore unavoidable [26].

At a linearized level, the metric of the spacetime could be written as a summation of the homogenous FRW metric $g_{\mu\nu}(t)$ and the unperturbed metric $\delta g_{\mu\nu}(t,x)$, that is $g_{\mu\nu}(t,x) = g_{\mu\nu}(t) + \delta g_{\mu\nu}(t,x)$. This perturbation contains 10 degrees of freedom which are decomposed in 4 scalars, 2 divergence-free vectors, and 2 trace-less and divergence-free tensors. Then the scalar metric perturbation can be written in term of the line-element as

$$ds^2 = a(\tau)^2 \left[-(1+2A)d\tau^2 + 2\partial_i B d\tau dx^i - (1-2\psi)\delta_{ij} - 2\partial_i\partial_j E dx^i dx^j\right], \quad (2.39)$$

where τ is the conformal time. Since the general relativity is a gauge theory where gauge transformations are the ones between local references, quantities defined in the unperturbed background are compared with those on the real physical spacetime at the same point. By fixing local references, comparison of two references leads to coordinate transformation $x^\mu \mapsto \tilde{x}^\mu = x^\mu + \xi^\mu$. As the result, every tensor, including the perturbations such as the metric perturbation, changes along the flow of a given vector field ξ^μ by an amount of Lie derivative of the tensor:

$$\delta\varphi \mapsto \delta\varphi + \mathcal{L}_\xi\varphi, \quad (2.40)$$

$$\delta g_{\mu\nu} \mapsto \delta g_{\mu\nu} + \mathcal{L}_\xi g_{\mu\nu}. \quad (2.41)$$

A quantity is preserved by the transformation of the references if its Lie derivative is vanish. As such examples, we have Bardeen's potentials Φ and Ψ:

$$\Phi := A + \mathcal{H}(B - E') + (B - E')', \quad \Psi := -C - \mathcal{H}(B - E'), \tag{2.42}$$

where $\mathcal{H} := a'/a$ and a prime denotes a derivative with τ. This $\mathcal{H}(\tau)$ is analogous with the Hubble parameter $H(t)$ in the cosmological time. The gauge invariance allows us to choose $A = \Phi$ and $\psi = -\Psi$ while $B = E = 0$, which is so called longitudinal gauge. The perturbed metric therefore can be written as

$$ds^2 = a(\tau)^2 \left[-(1 + 2\Phi)d\tau^2 + (1 - 2\Psi)\delta_{ij}dx^i dx^j\right]. \tag{2.43}$$

Evaluation of the perturbed Einstein equation with $\delta G^\mu_\nu = \kappa^2 \delta T^\mu_\nu$, where $\kappa^2 := 8\pi G = 1/M^2_{\rm pl}$, gives

$$\nabla^2\Phi - 3\mathcal{H}\left(\mathcal{H}\Phi + \Phi'\right) = \frac{\kappa^2}{2}\left(\varphi_0'\delta\varphi' - \varphi_0'^2\Phi + a^2\partial_\varphi V(\varphi)\delta\varphi\right), \tag{2.44}$$

$$\Phi' + \mathcal{H}\Phi = \frac{\kappa^2}{2}\varphi_0'\delta\varphi, \tag{2.45}$$

$$\Phi'' + 3\mathcal{H}\Phi' + \left(2\mathcal{H}' + \mathcal{H}^2\right)\Phi = \frac{\kappa^2}{2}\left(\varphi_0'\delta\varphi' - \varphi_0'^2\Phi - a^2\partial_\varphi V(\varphi)\delta\varphi\right). \tag{2.46}$$

φ_0 represents the unperturbed field component. The spatial component of the perturbed Einstein equation leads to a relation $\Psi = \Phi$.

Spatial curvature on the hypersurface of a constant conformal time for the flat universe is given by ${}^{(3)}R = \frac{4}{a^2}\nabla^2\psi$. On a different slice, where the time is transformed to $t \mapsto t + \delta\tau$, the curvature perturbation ψ changes as $\psi \mapsto \psi + \mathcal{H}\delta\tau$. For a comoving observer, who only perceives the universe to be isotopic, a variation of φ would be detected as $\delta\varphi_{\rm com} = 0$. As a result, the transformation on constant time hypersurface $\delta\varphi \mapsto \delta\varphi - \varphi'\delta\tau$ leads to the time displacement $\delta\tau = \delta\varphi/\varphi'$ which corresponds to the transformation from a slice with the generic $\delta\varphi$ to a comoving slice orthogonal to the comoving observer. Thus, the curvature perturbation on the

comoving hypersurfaces can be written as

$$\mathcal{R} := \psi \mid_{\delta\varphi=0} = \psi - \frac{\mathcal{H}}{\varphi'}\delta\varphi = \psi - H\frac{\delta\varphi}{\dot{\varphi}} \tag{2.47}$$

$$= \Phi - \frac{H^2}{\dot{H}}\left(\Phi - \frac{\dot{\Phi}}{H}\right). \tag{2.48}$$

The second equation could be obtained by adopting equation (2.45) and the relation $\Psi = \Phi$ obtained from the spatial component of the perturbed Einstein equation. This intrinsic curvature perturbation $\mathcal{R}$ is also gauge invariant as it is given entirely in terms of the gauge-invariant quantities. This quantity is constant on each scale on the outside of the horizon. Thus, its spectrum gives the curvature perturbation amplitude of different modes when they cross into the Hubble radius during the matter or radiation dominated epoch. Fourier expansion of $\mathcal{R}$ and its vacuum expectation value are given as

$$\mathcal{R} = \int \frac{d^3\mathbf{k}}{(2\pi)^{3/2}}\mathcal{R}_{\mathbf{k}}(\tau)e^{i\mathbf{k}\cdot x}, \quad \langle \mathcal{R}_{\mathbf{k}}\mathcal{R}^*_{\mathbf{k}'}\rangle = \frac{2\pi^2}{k^3}\mathcal{P}_{\mathcal{R}}(k)\delta^3(\mathbf{k}-\mathbf{k}'), \tag{2.49}$$

respectively. $\mathcal{P}_{\mathcal{R}}(k)$ is known as the spectrum of comoving curvature perturbation. It depends only on the magnitude of the wave number.

Quantum fluctuations during inflation are the source of large scale structure of the universe observed today. Therefore, studying of the quantization of the perturbations is required to understand it correctly. Canonical commutation relation between the scalar field perturbation and its canonical conjugate than needs to be defined. To do so, one can start from the total action of the scalar field and the gravitational field and then expand it up to the second order of the perturbations. We find it as

$$S = \frac{1}{2}\int d^3\mathbf{x}d\tau\left((v')^2 - (\partial_i v)^2 + \frac{z''}{z}v^2\right) \tag{2.50}$$

where v and z are defined by $v := -z\mathcal{R}$ and $z := a\dot{\varphi}/H$ [46]. It is a kind of free scalar field action with a time dependent effective mass term $m^2(\tau) = -z''/z$. In terms of the slow roll approximation, z can be written as $z^2 = 2a^2\varepsilon^2$. Therefore,

z''/z can be exactly expressed as

$$\frac{z''}{z} = a^2H^2\left[2-\varepsilon+\frac{3}{2}\eta-\frac{1}{2}\varepsilon\eta+\frac{1}{4}\eta^2+\eta\kappa\right], \tag{2.51}$$

where we used $\varepsilon := -\frac{\dot{H}}{H^2}, \eta := \frac{\dot{\varepsilon}}{H\varepsilon}$ and $\kappa := \frac{\dot{\eta}}{H\eta}$. As $\frac{d}{d\tau}(aH)^{-1} = \varepsilon - 1$, we can obtain the first order approximation of z''/z as

$$\frac{z''}{z} \simeq \frac{\nu^2-(1/4)}{\tau^2}, \quad \nu := \frac{3}{2}+\varepsilon+\frac{1}{2}\eta. \tag{2.52}$$

It shows how the effective mass $m^2(\tau) \simeq z''/z$ depends on the conformal time τ or the comoving Hubble radius $(aH)^{-1}$.

Canonical conjugate of v can be found from equation (2.50) as $\pi_v = \frac{\partial\mathcal{L}}{\partial v'} = v'$. Quantization of the theory means to promote the classical variables $\{v, \pi_v\}$ to the quantum operators $\{\hat{v}, \hat{\pi}_v\}$ so that they satisfy the following commutation relations:

$$\begin{aligned}[\hat{v}(\tau,\mathbf{x}), \hat{\pi}_v(\tau,\mathbf{x}')] &= i\delta^3(\mathbf{x}-\mathbf{x}'),\\ [\hat{v}(\tau,\mathbf{x}), \hat{v}(\tau,\mathbf{x}')] &= [\hat{\pi}_v(\tau,\mathbf{x}), \hat{\pi}_v(\tau,\mathbf{x}')] = 0.\end{aligned} \tag{2.53}$$

If the operator $\hat{v}(\tau,\mathbf{x})$ is expanded with the plane waves basis which is one of complete solutions of the classical equation of motion (2.50), we have

$$\hat{v}(\tau,\mathbf{x}) = \int \frac{d^3\mathbf{k}}{(2\pi)^{3/2}}\left(v_k\hat{a}_\mathbf{k}e^{i\mathbf{k}\cdot\mathbf{x}} + v_k^*\hat{a}_\mathbf{k}^\dagger e^{-i\mathbf{k}\cdot\mathbf{x}}\right) \tag{2.54}$$

where $v_k = v_k(\tau)$ are complex and time dependent coefficients. To satisfy standard commutation relation between the creation and annihilation operators $\hat{a}^\dagger$ and $\hat{a}$, the normalization condition for the coefficient $v_k(\tau)$ requires

$$v_k'(\tau)v_k^*(\tau) - v_k^{*'}(\tau)v_k(\tau) = 2i. \tag{2.55}$$

The vacuum $|0\rangle$ can now be defined as the state which is annihilated by all $a_\mathbf{k}$, such as $a_\mathbf{k}|0\rangle = 0$.

The minimal action principle for equation (2.50) produces the equation of motion for v_k as follows

$$v_k'' + (k^2 - \frac{z''}{z})v_k = 0. \tag{2.56}$$

Inside the horizon where $k/aH \to \infty$ is satisfied, the contribution of the time-dependent effective mass term z''/z is negligible in this equation. Thus, v_k has a solution in the small wavelength limit such as

$$\lim_{\frac{k}{aH}\to\infty} v_k = \frac{1}{\sqrt{2k}} e^{ik\tau}. \tag{2.57}$$

This can be a good initial condition to solve equation (2.56). In the approximation that the slow-roll parameters are constant in time, this equation has a general solution in terms of the first and second kind of Hankel functions $H_\nu^{(1)}$ and $H_\nu^{(2)}$ as

$$v_k(\tau) = \sqrt{-\tau}\left[\alpha H_\nu^{(1)}(-k\tau) + \beta H_\nu^{(2)}(-k\tau)\right]. \tag{2.58}$$

Imposing the boundary condition (2.57) at the asymptotic limit inside the horizon, the linear combination coefficients in the general solution of v_k should be normalized to be $\alpha = \frac{\sqrt{\pi}}{2} e^{i(\nu+\frac{1}{2})\frac{\pi}{2}}$ and $\beta = 0$. Thus the resulting expression of v_k inside the horizon is given as

$$v_k(\tau) = \sqrt{\frac{\pi}{2}}(-\tau)^{1/2} e^{i(\nu+\frac{1}{2})\frac{\pi}{2}} H_\nu^{(1)}(-k\tau). \tag{2.59}$$

On the other hand, the solution outside of the horizon is given in large wavelength $k/aH \to 0$ limit of equation (2.58) as

$$\lim_{\frac{k}{aH}\to 0} v_k = e^{i(\nu-\frac{1}{2})\frac{\pi}{2}} 2^{\nu-\frac{3}{2}} \frac{\Gamma(\nu)}{\Gamma(3/2)} \frac{1}{\sqrt{2k}} (-k\tau)^{\frac{1}{2}-\nu}, \tag{2.60}$$

where we have used $\lim_{\frac{k}{aH}\to 0} H_\nu^{(1)}(-k\tau) = \frac{i}{\pi}\Gamma(\nu)\left(\frac{-k\tau}{2}\right)^{-\nu}$ and $\sqrt{\pi}/2 = \Gamma(3/2)$ in the equation. Since v_k is related to $\mathcal{R}_k$ as $v_k = -z\mathcal{R}_k$, the power spectrum of comoving

curvature perturbation in equation (2.49) can be expressed as

$$\mathcal{P}_{\mathcal{R}} = 2^{2\nu-3}\left(\frac{\Gamma(\nu)}{\Gamma(3/2)}\right)^2(1-\varepsilon)^{2\nu-1}\left(\frac{H}{2\pi}\right)^2\left(\frac{H}{\dot{\varphi}}\right)^2\left(\frac{k}{aH}\right)^{3-2\nu}. \tag{2.61}$$

This expression shows how the power spectrum stays constant outside the horizon during the time when the slow-roll approximation is valid. Thus, we can choose to evaluate it at the time when the scale k exits the horizon, i.e $k = aH$. The slow-roll parameters for each k are kept their values at horizon exit so that to produce a general solution given in equation (2.58), even though they may change significantly afterward. Scale dependance of the power spectrum $\mathcal{P}_{\mathcal{R}}$ is expressed in terms of the spectral index of the comoving curvature perturbation n_s, given by

$$n_s - 1 := \frac{d\ln\mathcal{P}_{\mathcal{R}}}{d\ln k} = 3 - 2\nu = -6\varepsilon + 2\eta \tag{2.62}$$

where the last equality is obtained from the first order slow-roll approximation for $k = aH$. Due to the smallness of the slow-roll parameters, the spectral index of the curvature perturbation may slightly deviate from which corresponds to the scale invariant $n_s = 1$. Taking account of $\nu \simeq 3/2$, the power spectrum $\mathcal{P}_{\mathcal{R}}$ can be compactly written as

$$\mathcal{P}_{\mathcal{R}}(k) = \Delta^2_{\mathcal{R}}\left(\frac{k}{aH}\right)^{n_s-1}, \quad \Delta^2_{\mathcal{R}} := \mathcal{P}_{\mathcal{R}}(k=aH) = \left.\frac{V}{24\pi^2 M_{pl}^4\varepsilon}\right|_{k=aH}. \tag{2.63}$$

The dependence of the spectral index on the scale is defined through the running of the spectral index

$$n_s' := \left.\frac{dn_s}{d\ln k}\right|_{k=aH} \simeq 16\varepsilon\eta - 24\varepsilon^2 - 2\xi. \tag{2.64}$$

where ξ is defined as $\xi := M_{pl}^4 V'V'''/V^2$.

The procedure to compute the quantum fluctuation of the scalar perturbation is also applicable to those of the tensor perturbations. Linear tensor perturbation of the background metric is given by transverse and traceless perturbation of spatial metric $\delta g_{ij} = a^2(\tau)h_{ij}$, where $|h_{ij}| \ll 1$ is satisfied. This fluctuation may be detected as the gravitational wave in the background spacetime. The symmetrical

spatial tensor h_{ij} has six degrees of freedom originally. They are reduced two degrees of freedom or polarizations by the traceless condition $\delta^{ij}h_{ij}$ and the transverse condition $h_{ij,k} = 0(k = 1, 2, 3)$. As the 3-tensor h_{ij} is gauge-invariant, the calculation could be simplified. Expansion of the Einstein-Hilbert action containing tensor perturbations is given in the second-order action as

$$S = \frac{M_{pl}}{8} \int d^3\mathbf{x} d\tau a^2 \left[(h'_{ij})^2 - (\nabla h_{ij})^2 \right]. \tag{2.65}$$

This is found to be similar to the massless scalar field action in a flat space by including the prefactor $M_{\rm pl}/2$ in the redefinition of the scalar field. We define Fourier expansion of the transverse and traceless tensor as

$$h_{ij}(\tau, \mathbf{x}) = \int \frac{d^3\mathbf{k}}{(2\pi)^{3/2}} \sum_{\lambda=1}^{2} h_{\mathbf{k},\lambda}(\tau) \epsilon^{\lambda}_{ij}(k) e^{i\mathbf{k}\cdot\mathbf{x}} \tag{2.66}$$

where $\epsilon^{\lambda}_{ij}(k)$ is a time-independent polarization tensor that naturally satisfies the same conditions as h_{ij}: symmetric, traceless ($\delta^{ij}\epsilon_{ij} = 0$) and transverse ($k^i\epsilon_{ij} = 0$). These polarization tensor need to be linearly independent and orthogonal $\epsilon^{\lambda}_{ij}\epsilon^{\lambda'*}_{ij} = \delta'_{\lambda\lambda}$. To simplify the calculation, we can choose a condition $\epsilon^*_{ij}(\mathbf{k}, \lambda) = \epsilon_{ij}(-\mathbf{k}, \lambda)$. A field redefinition $v_{\mathbf{k},\lambda} := \frac{M_{pl}}{2} a h_{\mathbf{k},\lambda}$ changes the tensor perturbations action (2.65) to

$$S = \sum_{\lambda=1}^{2} \frac{1}{2} \int d^3\mathbf{k} d\tau \left[\left(v'_{\mathbf{k},\lambda}\right)^2 - \left(k^2 - \frac{a''}{a}\right) \left(v_{\mathbf{k},\lambda}\right)^2 \right]. \tag{2.67}$$

To quantize the field $v_{\mathbf{k},\lambda}$, the scalar modes $v_k(\tau)$ introduced in the quantization of the scalar fluctuation can be used. For this purpose, we introduce creation and annihilation operators $\hat{a}_{\mathbf{k},\lambda}$ and $\hat{a}^{\dagger}_{\mathbf{k},\lambda}$ which satisfy the commutation relations $\left[\hat{a}_{\mathbf{k},\lambda}, \hat{a}^{\dagger}_{\mathbf{k}',\lambda'}\right] = \delta^3(\mathbf{k} - \mathbf{k}')\delta_{\lambda\lambda'}$ and $[\hat{a}_{\mathbf{k},\lambda}, \hat{a}_{\mathbf{k}',\lambda'}] = \left[\hat{a}^{\dagger}_{\mathbf{k},\lambda}, \hat{a}^{\dagger}_{\mathbf{k}',\lambda'}\right] = 0$. If we use them, operator of $v_{\mathbf{k},\lambda}$ is written as

$$\hat{v}_{\mathbf{k},\lambda} = v_k \hat{a}_{\mathbf{k},\lambda} + v^*_k \hat{a}^{\dagger}_{\mathbf{k},\lambda}. \tag{2.68}$$

Minimal action principle for (2.67) produces a similar equation as (2.56):

$$v_k'' + \left(k^2 - \frac{a''}{a}\right) = 0, \tag{2.69}$$

where the term z''/z in equation (2.56) is replaced by a factor $a''/a = 2a^2H^2(1 - (\varepsilon/2)) = \tau^{-2}(\mu^2 - (1/4))$, where $\mu = (1-\varepsilon)^{-1} + (1/2) \simeq (3/2) + \varepsilon$. As in the scalar case, a solution for the scale k inside the horizon is given by applying the boundary condition $\lim_{k/aH\to\infty} v_k = e^{ik\tau}/(\sqrt{2k})$, which be used as condition for its general solution. Tensor power spectrum $\mathcal{P}_T$ could be defined through the quantum vacuum fluctuations

$$\sum_{\lambda=1}^{2} \left\langle h_{\mathbf{k},\lambda}, h^{\dagger}_{\mathbf{k}',\lambda} \right\rangle := \frac{2\pi^2}{k^3}\mathcal{P}_T\delta^3\left(\mathbf{k}-\mathbf{k}'\right) = 2 \times \frac{4\left|v_k\right|^2}{M_{pl}^2 a^2}\delta^3\left(\mathbf{k}-\mathbf{k}'\right), \tag{2.70}$$

where the factor 2 comes from two possible polarization states of $h_{\mathbf{k},\lambda}$. Thus, the tensor power spectrum has an expression outside of the horizon as

$$\mathcal{P}_T = \frac{8}{M_{pl}^2} 2^{2\mu-3} \left(\frac{\Gamma(\mu)}{\Gamma(3/2)}\right)^2 (1-\varepsilon)^{2\mu-1} \left(\frac{H}{2\pi}\right)^2 \left(\frac{k}{aH}\right)^{3-2\mu}, \tag{2.71}$$

which always can be chosen to be evaluated at $k = aH$ since it is freeze after the horizon exit. If $\mu \simeq 3/2$ is satisfied, it leads to the scale dependent expression. The tensor power spectrum can be expressed as

$$\mathcal{P}_T(k) = \Delta_T^2 \left(\frac{k}{aH}\right)^{n_T}, \quad \Delta_T^2 := \mathcal{P}_T(k=aH) = \frac{8}{M_{pl}^2}\left(\frac{H}{2\pi}\right)^2\Bigg|_{k=aH}, \tag{2.72}$$

where n_T denotes the spectral index of the tensor perturbation and it is defined as

$$n_T := \frac{d\ln\mathcal{P}_T}{d\ln k} = 3 - 2\mu = -2\varepsilon. \tag{2.73}$$

Since $\varepsilon \ll 1$ is satisfied until end of inflation, it shows that the spectrum of tensor perturbation is almost scale invariant. It is also important to notice that the amplitude of the tensor perturbation Δ_T^2 only depends on the value of the Hubble parameter during inflation which is proportional to the energy scale $V^{1/4}$ of inflation. Therefore, a detection of the gravitational wave provides a direct detection of

the energy scale of inflation.

Ratio of the tensor power spectrum to the scalar power spectrum is known as the tensor-to-scalar ratio r. This quantity is expressed as

$$r := \frac{\mathcal{P}_T}{\mathcal{P}_\mathcal{R}} \simeq 16\varepsilon = -8n_T. \tag{2.74}$$

This prediction is only satisfied by the single field inflation model in the slow-roll approximation treatment. Different models of inflation might bring different predicted relation. Thus, if the detection of CMB anisotropy does not fulfill this condition, it does not mean that inflation does not exist. One need only to consider a different model of inflation which contains more than one field or a different inflation realization as mentioned in the previous section. The tensor-to-scalar ratio r, spectral index n_s and its running n_s' are observables detected through the CMB anisotropy measurement such as Planck and Bicep2 experiments.

2.4 Lyth bound and η problem

To predict a detectably-large primordial gravitational wave signal, inflationary models should be very sensitive to ultraviolet physics. This condition is known as the Lyth bound. It expresses a relation between observational constraints on the tensor modes and the field variation during inflation. A large tensor-to-scalar ratio given by recent experiments requires the super-Planckian inflaton displacement [16, 47]. Let consider single field slow-roll inflation caused by the inflaton φ. In such a case, by substituting the slow-roll parameter $\varepsilon = -\dot{H}/H^2$ to $r = 16\varepsilon$ we get a relation between the tensor-to-scalar ratio and the variation of the inflaton as

$$r = 8\left(\frac{1}{M_{\rm pl}}\frac{d\varphi}{dN}\right), \tag{2.75}$$

where N is the e-folding number. Integration of this equation from the time of the horizon exit N_* to the end of inflation $N_e := 0$ leads to

$$\frac{\Delta\varphi}{M_{\rm pl}} = N_{\rm eff}\sqrt{\frac{r_*}{8}}, \quad N_{\rm eff} := \int_0^{N_*} dN\sqrt{\frac{r}{8}}, \tag{2.76}$$

where r_* denotes the value of the tensor-to-scalar ratio measured in the CMB and $\Delta\varphi$ is the corresponding variation of inflaton. In slow-roll inflation, one can find a relation

$$\frac{d\ln r}{dN} = \left[n_s - 1 + \frac{r}{8}\right]. \tag{2.77}$$

Thus, $N_{\rm eff}$ can be evaluated in terms of the observed values r and n_s. However, $N_{\rm eff}$ could be effectively approximated as the number of e-folding before the end of inflation. Thus, the standard estimation gives $N_{\rm eff} < 60$. Lyth [16] pointed out that its lowest bound is obtained as the one that the scales $1 < l \lesssim 100$ leave the horizon. As $dN = Hdt \simeq d\ln a$, a detectable r requires $N_{\rm eff} > 0.46$, which shows that the variation of the inflaton during inflation requires

$$\Delta\varphi \gtrsim 4.6\sqrt{\frac{r_*}{8}}M_{\rm pl}. \tag{2.78}$$

As an example if we take $r = 0.1$, $\Delta\varphi \gtrsim 0.51 M_{\rm pl}$ is required. The Lyth bound arises because large r requires large ε. However, one can obtain a sufficient e-folding number even for the small field variation by assuming the small $\varepsilon(\varphi)$ because of the relation $dN/d\varphi = (2\varepsilon)^{-1/2}$. Therefore, if ε starts having large value initially and quickly goes to small value afterward, the Lyth bound might be circumvented. Unfortunately, the slow-roll parameter ε cannot vary arbitrarily in a way as

$$\frac{d\sqrt{2\varepsilon}}{d\varphi} = \eta - 2\varepsilon \ll 1 \tag{2.79}$$

during inflation [48]. Thus, the Lyth bound could not be evaded by any choice of the slow-roll inflaton potential, even if ε is not monotonous.

In more general inflation scenarios, such as inflation driven by the kinetic term, the Lyth bound is also manifest [49]. In such case, the standard slow-roll parameter and the tensor-to-scalar ratio are given as

$$\varepsilon = -\frac{\dot{H}}{H^2} = \frac{XP_{,X}}{M_{\rm pl}^2 H^2}, \tag{2.80}$$

$$r = 16 c_s \varepsilon, \tag{2.81}$$

where c_s defined by $c_s^2 := dp/d\rho = \frac{P_{,X}}{P_{,X}+2XP_{,XX}}$ plays the role of the speed of sound for perturbations [34]. The standard slow-roll prediction is recovered in the limit $c_s = 1$. Following previous procedure, the Lyth bound of this inflation scenario could be written as

$$\frac{\Delta\varphi}{M_{\rm pl}} = \int_0^{N_*} dN \sqrt{\frac{r}{8}\frac{1}{c_s P_{,X}}}. \tag{2.82}$$

Thus, for a naive bound $\frac{\Delta\varphi}{M_{\rm pl}} = \Delta N\sqrt{\frac{r}{8}\frac{1}{c_s P_{,X}}}$, it requires $P_{,X} \gg 1$ to avoid the Lyth bound for fix c_s. This technically leads to $X \ll 1$ to guarantee the inflation. As a result, the model merely moves to the slow-roll inflation class in which the Lyth bound could not be avoided.

A possible way to evade this Lyth bound is by considering inflation scenario produced by a large number N of inflaton fields [50–52]. By applying the Pythagorean theorem, each constituent field only needs a short field variation $\Delta\phi_i \sim \Delta\phi/\sqrt{N}$ to realize such large field variation $\Delta\phi$ required by the Lyth bound. The other way is by imposing the allowed field trajectory in a small area with a radius less than $M_{\rm pl}$ [53–55]. The length of the trajectory in a such scenario is large enough to evade the Lyth bound.

The reason behind importance of the Lyth bound is related to the UV completion theory of the inflationary model. If the inflation can be approximately described as low energy limit of more fundamental theories such as supergravity or string theory by integrating out high momentum degrees of freedom, the effective field theory description of the inflation involves an effective potential for the inflaton [47, 56]

$$V(\varphi) = V_0(\varphi) + \sum_i c_i \frac{\mathcal{O}_i(\varphi)}{\Lambda^{\delta_i-4}}. \tag{2.83}$$

where $\mathcal{O}_i$ is local operator of dimension δ_i and Λ a cutoff scale. Once the inflaton becomes super-Planckian taking $\Lambda = M_{\rm pl}$, nonrenormalizable terms $\delta_i > 4$ could not be under control and have significant contributions to the potential. In such case, flatness of the potential might be ruined and the slow-roll condition could not

be realized. In the context of effective field theory, considering the operator

$$\mathcal{O}_\delta = cV_0(\varphi)\left(\frac{\varphi}{\Lambda}\right)^{\delta-4}, \tag{2.84}$$

the correction $\Delta\eta$ to the slow-roll parameter η can be calculated as

$$\Delta\eta \simeq c(\delta-4)(\delta-5)\left(\frac{\varphi}{\Lambda}\right)^{\delta-6} \tag{2.85}$$

Thus, if we take $\Lambda = M_{\rm pl}$, and φ as a trans-Planckian field, then the correction cannot be neglected for $\delta \geq 6$ to suffer the violation of $\eta \ll 1$. This condition is known as η problem.

Chapter 3

Modification of The Radiative Neutrino Mass Generation Model

3.1 Neutrino masses

Fermion mass term can be introduced in the Lagrangian via so called Higgs mechanism. In this mechanism, gauge symmetry of the Lagrangian is hypothetically broken spontaneously by an existence of non-zero vacuum expectation value (VEV) of a scalar field named Higgs field. The main consequence of this spontaneous symmetry breaking is that a Yukawa coupling such as $Y\bar{\psi}\tilde{\phi}\psi$ will generate fermion mass term $Yv\bar{\psi}\psi := m\bar{\psi}\psi$ after Higgs field ϕ gets vacuum expectation value (VEV) $\langle\phi\rangle := v$.

If we impose chirality decomposition $\psi = \psi_L + \psi_R$ on the Lagrangian, only mixed terms remains

$$-\mathcal{L}_{mass} = m\bar{\psi}\psi = m\left(\bar{\psi}_L\psi_R + \bar{\psi}_R\psi_L\right). \tag{3.1}$$

This mass term is called Dirac mass term. In this context, any massive fermion field need to have both non-zero chiral field components. Neutrinos must therefore be massless as the standard model particle because they have no right handed components.

Alternatively, one could also introduce the so-called Majorana mass term, without needing to introduce the right handed degree of freedom. Majorana fermion is the one which is its own antifermion, $\psi^c = \psi$. This means that Majorana field should not have charge that is reversed by charge conjugation operator: electric charge, colour, lepton number and baryon number. Charge conjugation operator acts on the chiral fields as $(\psi_L)^c = (\psi^c)_R$ and $(\psi_R)^c = (\psi^c)_L$ so that Majorana field can be expressed in term of one chiral field component as

$$\psi = \psi_L + \psi_R = \psi_L + (\psi^c)_R = \psi_L + (\psi_L)^c. \tag{3.2}$$

This expression helps to develop non-zero mass term as

$$-\mathcal{L} = \frac{1}{2} m \bar{\psi^c} \psi + \text{h.c} \tag{3.3}$$

even without the existence of both chiral components as the independent ones.

3.2 Ma's Radiative neutrino mass model

Radiative seesaw scenario is an alternative way to explain tiny neutrino masses. In this scenario they are radiatively induced at the one loop level by imposing an exact Z_2 symmetry and introducing additional Z_2-odd scalar doublet η and Z_2-odd right-handed neutrino $N_i (i = 1, 2, 3)$ [57]. All of the standard model particle are labeled by even parity. As a result of this assignment, the right-handed neutrinos only have Yukawa couplings with the scalar $SU(2)_L$ doublet η and Yukawa couplings between η and standard model fermions are forbidden. It is a reason to call η as an inert $SU(2)_L$. doublet. Under $SU(2)_L \times U(1)_Y \times Z_2$, the particle contents relevant to the neutrino mass can be represented as follows [58]:

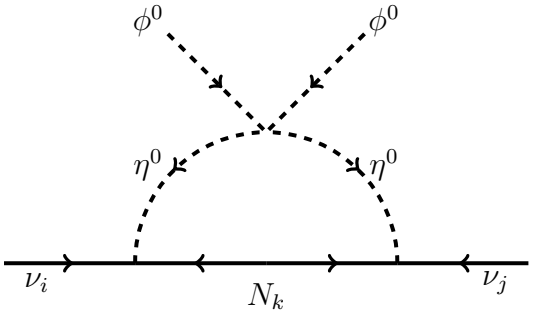

FIGURE 3.1: One-loop generation of neutrino mass considered in the radiative neutrino masses model with an inert doublet [58]

$$\begin{pmatrix} \nu_i \\ l_i \end{pmatrix} \sim (2, -1/2, +), \quad l_i^c \sim (1, 1, +), \quad \Phi := \begin{pmatrix} \phi^+ \\ \phi^0 \end{pmatrix} \sim (2, 1/2, +)$$
$$N_i \sim (1, 0, -), \quad \eta := \begin{pmatrix} \eta^+ \\ \eta^0 \end{pmatrix} \sim (2, 1/2, -) \tag{3.4}$$

If the Z_2 symmetry is exact, all of Lagrangian terms need to contain an even number of new fields. Hence, Yukawa coupling containing the right-handed neutrino, the SM Higgs doublet Φ and the left-handed lepton which is responsible to generate a Dirac mass term between ν_L and N_i is forbidden. On the other hand, coupling involving right-handed neutrino, the new scalar doublet η, and the left-handed lepton is allowed. However, once η^0 gets a non zero vacuum expectation value, the symmetry will be broken. The symmetry breaking pattern for all possible combination of the VEV's of ϕ^0 and η^0 has been analyzed in [59]. If the VEV of η^0 is zero and Z_2 is kept as the exact symmetry, there is no decay mode of the lightest Z_2-odd particle and it is stabilized. Thus, it can act as the dark matter as long as it is electrically neutral [57].

The Invariant Yukawa interactions with Majorana mass term of the model are summarized as

$$-\mathcal{L}_N = -h_{\alpha i}\bar{N}_i\eta^\dagger l_\alpha - h^*_{\alpha i}\bar{l}_\alpha\eta N_i + \frac{M_i}{2}\bar{N}_i N_i^c + \frac{M_i^*}{2}\bar{N}_i^c N_i \tag{3.5}$$

and the scalar sector potential is given as

$$\begin{aligned} V_{\text{scalar}} = \; & m_1^2 \Phi^\dagger \Phi + m_2^2 \eta^\dagger \eta + \lambda_1 (\Phi^\dagger \Phi)^2 + \lambda_2 (\eta^\dagger \eta)^2 \\ & + \lambda_3 (\Phi^\dagger \Phi)(\eta^\dagger \eta) + \lambda_4 (\Phi^\dagger \eta)(\eta^\dagger \Phi) \\ & + \frac{1}{2} \left[\lambda_5 (\Phi^\dagger \eta)^2 + \lambda_5^* (\Phi \eta^\dagger)^2 \right]. \end{aligned} \tag{3.6}$$

Any bilinear term $(\Phi^\dagger \eta)$ is forbidden by the Z_2 symmetry so that λ_5 can always be chosen as a real parameter by the field redefinition for η. Under the assumption that $m_1^2 < 0$ and $m_2^2 > 0$, Higgs Φ obtains the vacuum expectation value $v := \sqrt{-m_1^2/2\lambda_1} = \langle \phi_0 \rangle$. After the electroweak symmetry breaking due to this VEV, there remain four spin 0 particles, that is a physical Higgs boson h which resembles the SM Higgs boson, as well as the CP even one $\text{Re}(\eta^0) := \eta_R^0$, the CP odd one $\text{Im}(\eta^0) := \eta_I^0$ and a pair of charged one $\eta^\pm$ [60]. The mass of these physical scalars are given by:

$$\begin{aligned} m_h^2 &= 4\lambda_1 v^2, \\ m_{\eta^\pm}^2 &= m_2^2 + \lambda_3 v^2, \\ m_{\eta_R^0}^2 &= m_2^2 + (\lambda_3 + \lambda_4 + \lambda_5) v^2, \\ m_{\eta_I^0}^2 &= m_2^2 + (\lambda_3 + \lambda_4 - \lambda_5) v^2. \end{aligned} \tag{3.7}$$

It is obvious that λ_5 controls the mass splitting between η_R^0 and η_I^0 and also λ_4 controls the mass splitting between the charged state $\eta^\pm$ and the neutral states $\eta_{R,I}^0$. To ensure that the potential is bounded from below at tree level, the quartic couplings should satisfy stability condition [11]:

$$\lambda_{1,2} > 0, \quad \lambda_3 > -\sqrt{\lambda_1 \lambda_2}, \quad (\lambda_3 + \lambda_4 \pm \lambda_5) > -\sqrt{\lambda_1 \lambda_2}. \tag{3.8}$$

Neutrino mass is generated through the one loop diagram given by Fig 3.1. Two neutral Higgs fields which appear as external fields do not propagate but get VEV after the electroweak symmetry breaking. The mass of neutrino due to this diagram can be calculated as the first order quantum correction of neutrino propagator involving the exchange of η_R^0 and η_I^0 as illustrated by Fig 3.2.

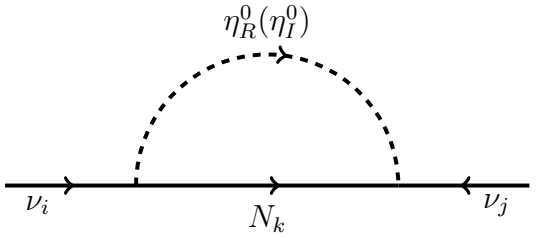

FIGURE 3.2: Neutrino mass correction in one-loop diagram involving the exchange of η^0

Applying Feynman rules to the diagram corresponding to the η_R^0 exchange gives:

$$-i\Sigma_{ij}^{\nu}(p) = \int \frac{d^4q}{(2\pi)^4}(-ih_{ik})\frac{i\left(\not{q}+M_k\right)}{q^2-M_k^2}(-ih_{kj})\frac{-i}{(p-q)^2-m_{\eta_R^0}^2} \tag{3.9}$$

$$= -\int \frac{d^4q}{(2\pi)^4}h_{ik}h_{kj}\frac{\not{q}+M_k}{(q^2-M_k^2)\left((p-q)^2-m_{\eta_R^0}^2\right)}. \tag{3.10}$$

This integral is logarithmically divergent since the numerator is proportional to $d^4q \simeq q^3dq$ while the denominator is proportional to q^4. At this point, we need to take care of the denominator by using Feynman parametrization to change $\left[(q^2-M_k^2)\left((p-q)^2-m_{\eta_R^0}^2\right)\right]^{-1} \to \int_0^1 dx\left[x\left(q^2-M_k^2\right)+(1-x)\left((p-q)^2-m_{\eta_R^0}^2\right)\right]^{-2}$ and using a regulation procedure to remove divergence in the loop integral. Since the neutrino masses are obtained as $\Sigma_{ij}^{\nu}(0)$, we take $p=0$. If we use the definition $\bar{q} := q - xp$ and $\Lambda_k^2 := \left(M_k^2 - m_{\eta_R^0}^2\right)x + m_{\eta_R^0}^2$, the one-loop integral can now be calculated as

$$\Sigma_{ij}^{\nu}(0) = \int_0^1 dx \int \frac{d^4\bar{q}}{i(2\pi)^4}\frac{M_k}{(\bar{q}^2-\Lambda_k^2)^2} = -\frac{M_k}{16\pi^2}\int_0^1 dx \log\frac{\Lambda_k^2}{\Lambda^2} \tag{3.11}$$

$$= \frac{M_k}{16\pi^2}\left[1+\frac{m_{\eta_R^0}^2}{M_k^2-m_{\eta_R^0}^2}\ln\left(\frac{m_{\eta_R^0}^2}{M_k^2}\right)+\ln\left(\frac{\Lambda^2}{M_k^2}\right)\right] \tag{3.12}$$

where Λ is a cut off. Calculation for the diagram corresponding to the η_I^0 exchange has a similar result, with extra minus term coming from the contraction of the field. Both contributions cancel the logaritmic divergence and yield the neutrino mass

matrix :

$$\mathcal{M}^{\nu}_{ij} = \frac{h_{ik}h_{kj}}{16\pi^2} M_k \left[\frac{m^2_{\eta^0_R}}{m^2_{\eta^0_R} - M^2_k} \ln\left(\frac{m^2_{\eta^0_R}}{M^2_k}\right) - \frac{m^2_{\eta^0_I}}{m^2_{\eta^0_I} - M^2_k} \ln\left(\frac{m^2_{\eta^0_I}}{M^2_k}\right) \right]. \tag{3.13}$$

where summation over index k is applied for the right-handed neutrino generation while i and j represent the neutrino generation index. If we use the quantities $\Delta m^2 := (m^2_{\eta^0_R} - m^2_{\eta^0_I})/2 = \lambda_5 v^2$ and $m_0^2 := (m^2_{\eta^0_R} + m^2_{\eta^0_I})/2$, the following approximate relations are obtained

$$\ln \frac{m_{\eta^0_R}}{M^2_k} = \ln\left(\frac{m_0^2 + \Delta m^2}{M^2_k}\right) \simeq \ln\left(\frac{m_0^2}{M^2_k}\right) + \frac{\Delta m^2}{m_0^2}, \tag{3.14}$$

$$\ln \frac{m_{\eta^0_I}}{M^2_k} = \ln\left(\frac{m_0^2 - \Delta m^2}{M^2_k}\right) \simeq \ln\left(\frac{m_0^2}{M^2_k}\right) - \frac{\Delta m^2}{m_0^2}. \tag{3.15}$$

If we assume $m_0^2 \gg \Delta m^2$, $m^2_{\eta^0_R} \simeq m^2_{\eta^0_I} \simeq m_0^2$ is satisfied and then neutrino mass equation becomes

$$\mathcal{M}^{\nu}_{ij} = \sum_{k=1}^{3} \frac{h_{ik}h_{kj}M_k}{8\pi^2} \frac{\lambda_5 v^2}{(m_0^2 - M^2_k)} \left[1 - \frac{M^2_k}{(m_0^2 - M^2_k)} \ln\left(\frac{m_0^2}{M^2_k}\right) \right]. \tag{3.16}$$

This equation shows that the smallness of λ_5 is a crucial role to explain the smallness of neutrino masses for the TeV range M_k and m_0.

The radiative neutrino mass model with an inert doublet is a promising candidate to explain phenomena beyond the Standard Model of particles such as the neutrino mass and mixing, the existence of dark matter and the baryon number asymmetry of universe [10]. In this model, baryogenesis could be associated with neutrino masses through a mechanism that relates the canonical seesaw mechanism and leptogenesis [61].

If the right-handed Majorana neutrino N_i with large mass M_i is added to the SM Lagrangian with Yukawa interaction $h_{i\alpha}\bar{N}^i_R l^\alpha_L \phi^\dagger$ + h.c, neutrino masses can be generated through the Weinberg dimension-five operator [62], $\frac{f_{\alpha\beta}}{2\Lambda}\left(l^\alpha_L \phi^\dagger\right)\left(l^\beta_L \phi^\dagger\right)$ + h.c. In fact in this model $\frac{f_{\alpha\beta}}{2\Lambda}$ is given as $\frac{f_{\alpha\beta}}{2\Lambda} := \sum_i h_{i\alpha}h_{i\beta}/M_i$ an neutrino masses are generated when the SM Higgs acquire the VEV $\langle\phi\rangle$. On the other side, since N_i decays into $l_L + \bar{\phi}$ or their antiparticles and the lepton number asymmetry could

be produced enough if neutrino masses M_i ar degenerated finally. This lepton number asymmetry at the early time of the universe, is converted into present baryon number asymmetry through sphalerons which cause electroweak vacuum states transition [63]. This is the famous leptogenesis scenario.

Unfortunately, Yukawa interaction containing the SM Higgs, the right-handed neutrino and the left-handed lepton doublet is forbidden in the radiative neutrino mass model with the inert doublet. However, there is Yukawa couplings $h_{\alpha i}\bar{N}_i\eta^\dagger l_\alpha$ + h.c that may mimic the role of $h_{i\alpha}\bar{N}_R^i l_L^\alpha\phi^\dagger$ + h.c mentioned before. Therefore, phenomena beyond the SM related with the neutrino masses and mixing and the baryon number asymmetry are expected to be explained well by the this model.

As it have been mentioned before, conservation of Z_2 in this model leads to stability of the lightest component of Z_2 odd field. As long as this field is neutral, it will be a good candidate of dark matter. Thus, there are two possible dark matter candidate in this model: the lightest neutral component of the inert doublet η_R^0 and the lightest right-handed neutrino N_i. If N_i is assumed as the cold dark matter, only two of three problems beyond the SM can be explain well [10, 64]. In such case, $O(1)$ Yukawa couplings are required to give a consistent explanation for the small neutrino masses and its relic abundance. On the other hand, such couplings allow to cause a large CP asymmetry in the decay of the right-handed neutrino. However, the same Yukawa couplings make the thermal leptogenesis fail to generate the sufficient lepton number asymmetry which is a seed of the baryon number asymmetry. Therefore, some extensions is required to explain those three problem [12]. For example, non-thermal leptogenesis, such as the generation of the lepton number asymmetry through inflaton decay, may need to be considered to take the place of the thermal leptogenesis [12]. Since the lepton number-violating effect could be separated from the DM sector, the reduction of the DM abundance and the washout of lepton number asymmetry might be reconciled for the same neutrino Yukawa couplings. In fact, if we choose the lightest neutral component as DM, those three of the problem beyond the SM could be explain well consistently even for the new fields with $O(1)$ TeV scale masses [65].

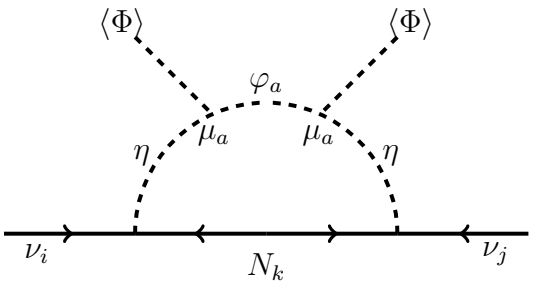

FIGURE 3.3: One-loop generation of neutrino masses in the present model. The coupling μ_a in this diagram is defined as $\mu_1 := \frac{\mu}{\sqrt{2}}$ and $\mu_2 := \frac{i\mu}{\sqrt{2}}$

3.3 Extending Ma-model

To explain the smallness of λ_5 in the Ma-model, we can consider a scenario in which this coupling is an effective coupling in low energy regions resulting from integrating out of a heavy singlet scalar S. In this scenario, the coupling λ_5 in the original model is supposed to be zero. We will explain how a λ_5 is derived from the extended model later. The new singlet scalar S should be a Z_2 odd field in order to couple with the inert doublet scalar η and Higgs doublet scalar Φ. The additional Lagrangian terms should be added in the Ma-model are

$$\begin{aligned} -\mathcal{L}_S = \quad & \tilde{m}_S^2 S^\dagger S + \frac{1}{2} m_S^2 S^2 + \frac{1}{2} m_S^2 S^{\dagger 2} \\ & + \kappa_1 \left(S^\dagger S\right)^2 + \kappa_2 \left(S^\dagger S\right)\left(\Phi^\dagger \Phi\right) + \kappa_3 \left(S^\dagger S\right)\left(\eta^\dagger \eta\right) \\ & - \mu S \eta^\dagger \Phi - \mu^* S^\dagger \Phi^\dagger \eta. \end{aligned} \tag{3.17}$$

Writing the singlet scalar S in its real components as $S = \frac{1}{\sqrt{2}}(\varphi_1 + i\varphi_2)$ and substituting to above equation, we can easily find the masses of these components are given as $\bar{m}_1^2 = \tilde{m}_S + m_S^2$ and $\bar{m}_2^2 = \tilde{m}_S^2 - m_S^2$. The potential containing S field does not develop the vacuum expectation value since Z_2 is considered to be an exact symmetry. Moreover, both of these field components masses are non negative, which requires κ_1 should be bounded from below. This requires $\tilde{m}_S^2 > m_S^2$.

Neutrinos still remain massless at tree level such as in the original Ma model since η has zero vacuum expectation value. Dirac neutrino masses cannot be generated through Yukawa coupling. However, neutrino masses can be generated through

diagram given in the Figure 3.3. By applying Feynman rules, the amplitude of this diagram is found to be

$$\mathcal{M} = h_{\alpha_i} h_{\beta i} \mu_a^2 \langle\Phi\rangle^2 \frac{I(p_1, p_2, p_3, M_i^2, m_1^2, m_2^2, m_3^2)}{16\pi^2}, \tag{3.18}$$

where μ_a is defined as $\mu_1 := \mu/\sqrt{2}$ and $\mu_2 := i\mu/\sqrt{2}$, respectively. The function $I(p_1, p_2, p_3, M_i^2, m_1^2, m_2^2, m_3^2)$ is defined as

$$\int d^4q \frac{(-i)^4(\not{q} + M_i)}{[q^2 - M_i^2]\,[(q+p_1)^2 - m_1^2]\,[(q+p_1+p_2)^2 - m_2^2]\,[(q+p_1+p_2+p_3)^2 - m_3^2]}, \tag{3.19}$$

where $m_1^2 = m_3^2 := M_\eta$ and $m_2^2 = \bar{m}_a^2, a = 1, 2$ and p_1, p_2, p_3 are external momentum of left handed neutrino and Higgs doublets respectively. M_η is mass of the inert doublet scalar η after the Higgs doublet gets the VEV and it is founded to be $M_\eta = m_\eta^2 + (\lambda_3 + \lambda_4)\langle\Phi\rangle^2$. The neutrino masses correction given by the amplitude (3.18) is obtained by putting all of the external momentum to be zero. Furthermore, The $\not{q}$-dependent part in the $I(p_1, p_2, p_3, M_i^2, m_1^2, m_2^2, m_3^2)$ will be integrated to zero because after Feynmann parametrization, the denominator will only depend on the magnitude of the internal momentum q but not depend on the its direction. The integral can be identified with the Passarino-Veltman function for a four-point function with vanishing external momentum $I(0, 0, 0, 0, M_i^2, m_1^2, m_2^2, m_3^2) := I(M_i^2, m_1^2, m_2^2, m_3^2)$ [66, 67] with a solution [68, 69] :

$$I(M_i^2, m_1^2, m_2^2, m_3^2) = \frac{1}{M_i^2 - m_1^2}\left[C_0\left(M_i^2, m_2^2, m_3^2\right) - C_0\left(M_i^2, m_2^2, m_3^2\right)\right], \tag{3.20}$$

where $C_0(m_a^2, m_b^2, m_c^2)$ is the three-point Passarino-Veltman function with vanishing external momentum given as

$$C_0(m_a^2, m_b^2, m_c^2) := \frac{1}{(m_a^2 - m_b^2)}\left[\frac{m_a^2}{m_a^2 - m_c^2}\ln\left(\frac{m_a^2}{m_c^2}\right) + \frac{m_b^2}{m_b^2 - m_c^2}\ln\left(\frac{m_b^2}{m_c^2}\right)\right]. \tag{3.21}$$

As a result, we have

$$I(M_i^2, m_1^2, m_2^2, m_3^2) = \frac{1}{M_i^2 - m_1^2}\left[\frac{M_i^2}{(M_i^2 - m_2^2)(M_i^2 - m_3^2)}\ln\left(\frac{M_i^2}{m_3^2}\right)\right.$$
$$- \frac{m_1^2}{(m_1^2 - m_2^2)(m_1^2 - m_3^2)}\ln\left(\frac{m_1^2}{m_3^2}\right)$$
$$\left. + \frac{m_2^2(m_1^2 - M_i^2)}{(m_1^2 - m_2^2)(m_2^2 - m_3^2)(M_i^2 - m_2^2)}\ln\left(\frac{m_2^2}{m_3^2}\right)\right]. \tag{3.22}$$

After taking a limit $m_3 \to m_1$, the quantity $I(M_i^2, m_1^2, m_2^2) := I(M_i^2, m_1^2, m_2^2, m_1^2)$ is written as

$$I(M_i^2, m_1^2, m_2^2) = -\frac{M_i^2\ln(M_i^2)}{(M_i^2 - m_2^2)(M_i^2 - m_1^2)^2} + \frac{(m_1^4 - M_i^2 m_2^2)\ln(m_1^2)}{(M_i^2 - m_1^2)^2(M_i^2 - m_2^2)^2}$$
$$+\frac{m_2^2\ln(m_2^2)}{(m_1^2 - m_2^2)^2(M_i^2 - m_2^2)} - \frac{1}{(M_i^2 - m_1^2)(m_1^2 - m_2^2)}. \tag{3.23}$$

Notes that the propagator of φ_a in the diagram of Figure 3.3 appears as a result of contraction between S and $S^\dagger$ so that each $\varphi_a, a = 1, 2$ contributes to the amplitude in equation (3.18) with a same sign and double the amplitude. The resulting neutrino mass matrix is written as

$$(\mathcal{M})_{\alpha\beta} = \sum_{i=1}^{3}\sum_{a=1}^{2}\frac{h_{\alpha_i}h_{\beta i}\mu_a^2\langle\Phi\rangle^2}{8\pi^2}I(M_i^2, M_\eta^2, \bar{m}_a^2). \tag{3.24}$$

This masses matrix is reduced to the neutrino masses matrix of Ma model given in the equation (3.16). In fact, assuming a condition that $\tilde{m}_S \gg m_S, m_\eta, M_i$, the approximated formula is given by

$$(\mathcal{M})_{\alpha\beta} = \sum_{i=1}^{3}\frac{h_{\alpha_i}h_{\beta i}\langle\Phi\rangle^2}{8\pi^2}\frac{m_S^2\mu^2}{\tilde{m}_S^4}\frac{M_i}{M_\eta^2 - M_i^2}\left[1 + \frac{M_i^2}{M_\eta^2 - M_i^2}\ln\left(\frac{M_i^2}{M_\eta^2}\right)\right], \tag{3.25}$$

where the factor $\frac{m_S^2\mu^2}{\tilde{m}_S^4}$ appears from $\sum_{a=1}^{2}\mu_a^2/\bar{m}^2$. Comparing this to equation (3.16), it is obvious that the coupling constant λ_5 for the $(\eta^\dagger\Phi)^2$ in the original model is effectively approximated as the quantity $\frac{m_S^2\mu^2}{\tilde{m}_S^4}$.

We might interpret the original model as the low energy limit of the present

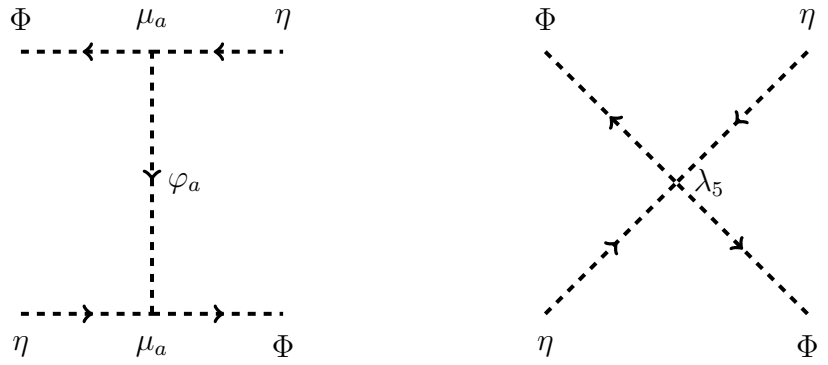

FIGURE 3.4: λ_5 as an effective coupling at energy regions much less than $\tilde{m}_S$.

extended model, in which λ_5 is an effective coupling derived from the interaction $-\mu S\eta^\dagger\Phi - \mu^* S^\dagger\Phi^\dagger\eta$ by integrating out S as shown in the Figure 3.4. At tree level of this extended model, the amplitude of the interaction $\eta\Phi \to \eta\Phi$ is given by

$$\mathcal{M} \simeq \left[\frac{\mu_1^2}{(q^2-\bar{m}_1^2)} - \frac{\mu_2^2}{(q^2-\bar{m}_2^2)}\right] \simeq \mu^2 \left[\frac{m_S^2}{\bar{m}_1^2\bar{m}_2^2}\right]_{\bar{m}_1^2,\bar{m}_2^2 \gg q^2} \simeq \frac{\mu^2 m_S^2}{\tilde{m}_S^4}, \tag{3.26}$$

which coincides with λ_5 in the original Ma model. Therefore, the corresponding terms in the energy regions much lower than $\tilde{m}_S^2$ are

$$\frac{1}{2}\left[\frac{m_S^2\mu^2}{\tilde{m}_S^4}(\eta^\dagger\Phi)^2 + \frac{m_S^2\mu^{*2}}{\tilde{m}_S^4}(\Phi^\dagger\eta)^2\right]. \tag{3.27}$$

Hierarchical masses problem between μ, m_S and $\tilde{m}_S$ now replaces the smallness problem of λ_5 in the Ma-model. It is a key factor to explain the smallness of the neutrino masses. If we leave the origin of this hierarchy problem to a complete theory at high energy regions, all the neutrino masses, the DM abundance and the baryon number asymmetry could be also explained in this extended model at TeV regions just as discussion given in [12].

Chapter 4

Aspects as The Inflation Model

4.1 The Inflation model

Following the proposal in [53], we consider an inflation scenario working at sub-Planckian scale by introducing nonrenormalizable terms obeying Z_2 symmetry to the potential for complex scalar field S given in equation (3.17). These terms could restrict the trajectory of the evolution of S. In that case, even though the radial motion of S is small, additional angular motion makes its whole trajectory length sufficiently large to evade the Lyth bound.

As such an example, lets assume that the complex scalar S has Z_2 invariant additional potential as below

$$V = c_1 \frac{\left(S^\dagger S\right)^n}{M_{\rm pl}^{2n-4}} \left[1 + c_2 \left(\frac{S}{M_{\rm pl}}\right)^{2m} \exp\left(i\frac{S^\dagger S}{\Lambda^2}\right) + c_2 \left(\frac{S^\dagger}{M_{\rm pl}}\right)^{2m} \exp\left(i\frac{S^\dagger S}{\Lambda^2}\right)\right] \quad (4.1)$$

$$= c_1 \frac{\varphi^{2n}}{2^n M_{\rm pl}^{2n-4}} \left[1 + 2c_2 \left(\frac{\varphi}{\sqrt{2}M_{\rm pl}}\right)^{2m} \cos\left(\frac{\varphi^2}{2\Lambda^2} + 2m\theta\right)\right], \quad (4.2)$$

where $M_{\rm pl}$ is the reduced Planck mass, and both of n and m are positive integers. In the second line, we adopt polar coordinate expression for $S = \frac{1}{\sqrt{2}}\varphi e^{i\theta}$. The most crucial part in the potential is the exponential term. However, we cannot explain its origin in this stage. We only expect that it might be effectively induced through

the nonperturbative dynamics in the UV completion of the model. In the Figure 4.1, we present typical shape of the potential when φ is varied for a fix θ value.

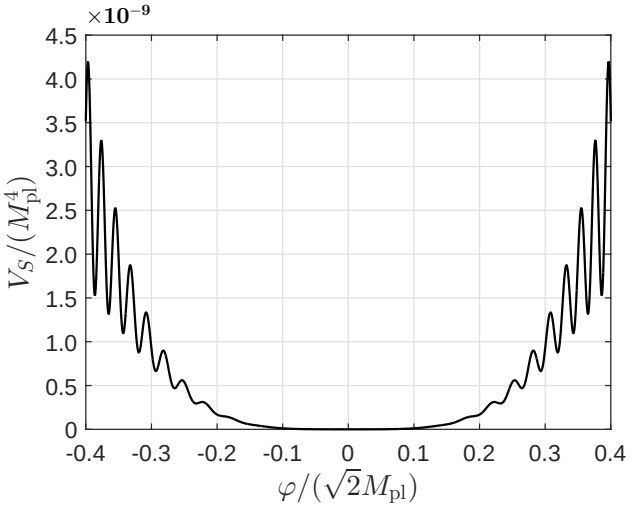

FIGURE 4.1: Potential shape for $n = 2, m = 1, c_1 = 1.1791 \times 10^{-7}, c_2 = 1.4$ and $\Lambda/M_{\rm pl} = 0.05$ when $\theta = 0$.

The local minimums of the potential can be obtained by finding the potential derivative of $V = V(\varphi, \theta)$. As the potential depends on two different variables, its minimums should be minimums for the both variables. Thus, at the potential minimums, derivatives along θ and φ satisfy the following conditions:

$$\frac{\partial V}{\partial \theta} = -4mc_1c_2M_{\rm pl}^4\phi\sin\psi = 0, \tag{4.3}$$

$$\frac{\partial V}{\partial \phi} = 2c_1M_{\rm pl}^4\phi^{n-1}\left[n + 2c_2(n+m)\phi^m\cos\psi - 2c_2\frac{M_{\rm pl}^2}{\Lambda^2}\phi^{m+2}\sin\psi\right] = 0. \tag{4.4}$$

Here, we temporally used

$$\phi := \left(\frac{\varphi}{\sqrt{2}M_{\rm pl}}\right), \quad \psi := \left(\frac{\phi^2}{(\lambda^2/M_{\rm pl}^2)} + 2m\theta\right) \tag{4.5}$$

to shorten and simplify the notation. Simultaneous solutions of above equations systems are related to conditions $\phi = 0$ or $\sin\psi = 0$. The first condition, $\phi = 0$, obviously describes the global minimum of the potential. On the other hand, by substituting the second condition $\sin\psi = 0$ to equation (4.1), it can be concluded that local potential minimums can be obtained only by taking $\cos\psi = -1$ but not

$\cos\psi = +1$. Thus, local minimums of V are located at

$$\frac{\varphi^2}{2\Lambda^2} + 2m\theta \simeq (2j+1)\pi \tag{4.6}$$

where j is an integer. Along this position, φ can be considered as a function of θ, $\varphi = \varphi(\theta)$ and the potential can be restricted as

$$V|_{min} \simeq V(\varphi) = c_1 M_{\rm pl}^4 \left(\frac{\varphi(\theta)}{\sqrt{2}M_{\rm pl}}\right)^{2n} \left[1 - 2c_2 \left(\frac{\varphi(\theta)}{\sqrt{2}M_{\rm pl}}\right)^{2m}\right]. \tag{4.7}$$

As a consequence of the smallness of the slow roll parameter η during inflation, inflaton mass should be small enough compared to Hubble parameter H. Therefore, any field having larger mass then Hubble parameter could not participate as inflaton. In case of field φ, its mass can be obtained from $dV(\varphi)^2/d\varphi^2$, that is given by

$$\begin{aligned} m_\varphi^2 &= \frac{d^2V(\varphi)}{d\varphi^2} = \frac{d\phi}{d\varphi}\frac{d}{d\phi}\left[\frac{d\phi}{d\varphi}\frac{dV(\varphi)}{d\phi}\right] \\ &= c_1 M_{\rm pl}^2 \left(\frac{\varphi}{\sqrt{2}M_{\rm pl}}\right)^{2n-2} \left[n(2n-1) - 2c_2(n+m)(2n+2m-1)\left(\frac{\varphi}{\sqrt{2}M_{\rm pl}}\right)^{2m}\right]. \end{aligned} \tag{4.8}$$

As long as φ is in the sub-Planckian domain ($\varphi < M_{\rm pl}$) and $c_2 = \mathcal{O}(1)$, the last line in the previous equation can be estimated as

$$m_\varphi \gtrsim \left[\frac{c_1}{2}n(2n-1)\right]^{1/2} \left(\frac{\varphi}{M_{\rm pl}}\right)^{n-2} \varphi. \tag{4.9}$$

On the other hand, the Hubble parameter is slowly changing during the inflation stage

$$H \simeq \left(\frac{V(\varphi)}{3M_{\rm pl}^2}\right)^{1/2} \simeq \left(\frac{c_1}{3\cdot 2^n}\right)^{1/2} \left(\frac{\varphi}{M_{\rm pl}}\right)^{n-1} \varphi. \tag{4.10}$$

As long as we keep φ in the sub-Planckian domain, the mass of φ will be much larger than the Hubble parameter and therefore cannot participate in the inflation

as inflaton. As the result, even thought the model originally consists of two degree of freedom, the model effectively behaves as a single field inflation model.

Now we assume that the inflaton a proceeds along the local minimums shown in equation (4.6). In that case, both of θ and φ fields vary its values when inflaton rolls downward from its initial point. The helical trajectory for the infinitesimal fields change shows variations given by

$$\frac{d\varphi}{d\theta} = -2m\Lambda^2 \left(\frac{1}{\varphi}\right). \tag{4.11}$$

The field a along this motion has a field variation satisfying

$$da = \left[\varphi^2 + \left(\frac{d\varphi}{d\theta}\right)^2\right]^{1/2} d\theta = \left[1 + 4m^2 \left(\frac{\Lambda}{\varphi}\right)^4\right]^{1/2} \varphi d\theta. \tag{4.12}$$

Therefore, inflaton a can be expressed as $da \simeq \varphi d\theta$ as long as the condition $\varphi \gg \Lambda$ is satisfied. In this case, we can consider a to be a canonically normalized field along the potential minimums. If we combine both condition $\varphi < M_{\rm pl}$ and $\varphi \gg \Lambda$, the assumption to take a as effective inflaton in this scenario is founded to be justified for $\Lambda \ll \varphi < M_{\rm pl}$. The eta problem is now transferred into the following in this model: (i) the condition $\Lambda/M_{\rm pl} \ll 1$, and (ii) hierarchical structure $\tilde{m}_S^2, m_S^2, \kappa_1\Phi^2 \ll H^2$ required by the domination (4.7) over the potential (4.1) during inflation. These η problem is remaining as long as the UV completion of the theory is not founded to fix the exponential terms in the potential (4.1). Meanwhile, the second form of the present η problem could be relevant with other low energy physics, such as the neutrino masses which could be elaborated here. Thus, the η problem is now partially described by neutrino masses generation and physics related with it.

Using $da = \varphi d\theta$, the change of the inflaton a from some period to the end of inflation can be expressed as

$$\begin{aligned} a_e - a &= -\int_{\varphi}^{\varphi_e} \varphi(\theta) d\theta = -\int_{\varphi}^{\varphi_e} \varphi \left(\frac{d\theta}{d\varphi}\right) d\varphi = \frac{1}{2m\Lambda^2} \int_{\varphi}^{\varphi_e} \varphi^2 d\varphi \\ &= \frac{1}{6m\Lambda^2} \left[\varphi_e^3 - \varphi^3\right], \end{aligned} \tag{4.13}$$

where φ_e is a value of φ at the end of inflation. If we define a canonically normalized new inflaton as

$$\chi := a_e + \frac{\varphi_e^3}{6m\Lambda^2} - a = \frac{\varphi^3}{6m\Lambda^2}, \tag{4.14}$$

it shows that we can promote χ to be super-Planckian field ($\chi \gg M_{\rm pl}$) even if φ is taken as a sub-planckian field. Therefore, the problem related to the Lyth bound can be evaded easily. In terms of this new field, the potential in equation (4.7) can be expressed as

$$V(\chi) = c_1 M_{\rm pl}^4 \left(\frac{3m\Lambda^2}{\sqrt{2}M_{\rm pl}^3}\right)^{2n/3} \chi^{2n/3} \left[1 - 2c_2 \left(\frac{3m\Lambda^2}{\sqrt{2}M_{\rm pl}^3}\right)^{2m/3} \chi^{2m/3}\right] \tag{4.15}$$

Since the leading contribution comes from the first term, our results are close to those given by the chaotic inflation with the power-low potential $V(\phi) = \Lambda^4 (\phi/M_{\rm pl})^p$ such as mentioned in [70, 71]. In this type of inflation model, the tensor-to-scalar ratio r increases with the power p, while the running of spectral index $|n_s'|$ decreases with the power p. Therefore, it is not easy to satisfy the BICEP2 and the Planck 2013 data, which give the constraints $r < 0.20$ (95% confidence) and $n_s' = -0.022 \pm 0.010$ (68% confidence for Planck+WP+highL data combination) [15, 72]. Unless the Planck and the BICEP2 data can be reconciled without large n_s', this chaotic inflation is inconsistent with the observation at the 1σ level. Since favorable results at the 95% confidence level are given for $2 < p < 3$, a reasonable choice in our model is to take $n = 3$ or $n = 4$ without including the running of the spectral index.

4.2 Constraints of slow-roll inflation

Quantities characterizing the inflation need to be calculated to understand the feature of the inflation. Some of them are the slow-roll parameters η and ε, the e-folding number N, the spectral index n_s, the tensor-to-scalar ratio r, the running of the spectral index n_s' and the power spectrum of the density perturbation $\mathcal{P}_\mathcal{R}$. In order to do so, the derivatives of the potential are needed. The first derivative of the

potential given in the equation (4.7) is

$$V' := \frac{dV(\chi)}{d\chi} = \left(\frac{d\varphi}{d\chi}\right)\frac{dV(\varphi)}{d\varphi} = c_1 M_{\rm pl}^4 \frac{\sqrt{2}m\Lambda^2}{M_{\rm pl}^3}\left(\frac{\varphi}{\sqrt{2}M_{\rm pl}}\right)^{2n-3} B(\varphi), \tag{4.16}$$

the second derivative is

$$V'' := \frac{d^2V(\chi)}{d\chi^2} = c_1 M_{\rm pl}^4 \frac{m^2\Lambda^4}{M_{\rm pl}^6}\left(\frac{\varphi}{\sqrt{2}M_{\rm pl}}\right)^{2n-6} C(\varphi), \tag{4.17}$$

and the third derivative

$$V''' := \frac{d^3V(\chi)}{d\chi^3} = c_1 M_{\rm pl}^4 \frac{m^3\Lambda^6}{\sqrt{2}M_{\rm pl}^9}\left(\frac{\varphi}{\sqrt{2}M_{\rm pl}}\right)^{2n-9} D(\varphi), \tag{4.18}$$

where we define

$$A(\varphi) := 1 - 2c_2\left(\frac{\varphi}{\sqrt{2}M_{\rm pl}}\right)^{2m}, \tag{4.19}$$

$$B(\varphi) := n - 2c_2(n+m)\left(\frac{\varphi}{\sqrt{2}M_{\rm pl}}\right)^{2m}, \tag{4.20}$$

$$C(\varphi) := n(2n-3) - 2c_2(n+m)(2n+2m-3)\left(\frac{\varphi}{\sqrt{2}M_{\rm pl}}\right)^{2m}, \tag{4.21}$$

$$D(\varphi) := n(2n-3)(2n-6) - 2c_2(n+m)(2n+2m-3)(2n+2m-6)\left(\frac{\varphi}{\sqrt{2}M_{\rm pl}}\right)^{2m}. \tag{4.22}$$

Using equation (4.7), (4.16), (4.17) and (4.18), the slow-roll parameters are now given by

$$\varepsilon := \frac{M_{\rm pl}^2}{2}\left(\frac{V'}{V}\right)^2 = m^2\left(\frac{\Lambda}{M_{\rm pl}}\right)^4\left(\frac{\varphi}{\sqrt{2}M_{\rm pl}}\right)^{-6}\left[\frac{B(\varphi)}{A(\varphi)}\right]^2, \tag{4.23}$$

$$\eta := M_{\rm pl}^2\left(\frac{V''}{V}\right) = m^2\left(\frac{\Lambda}{M_{\rm pl}}\right)^4\left(\frac{\varphi}{\sqrt{2}M_{\rm pl}}\right)^{-6}\left[\frac{C(\varphi)}{A(\varphi)}\right], \tag{4.24}$$

and

$$\xi := M_{\rm pl}^4 \frac{V'V'''}{V^2} = m^4 \left(\frac{\Lambda}{M_{\rm pl}}\right)^8 \left(\frac{\varphi}{\sqrt{2}M_{\rm pl}}\right)^{-12} \left[\frac{B(\varphi)D(\varphi)}{A(\varphi)^2}\right]. \tag{4.25}$$

These first two parameters give the condition for the period when the inflation is occurring. The inflation starts from the period when $\eta \ll 1$ and $\varepsilon \ll 1$ are satisfied and then stops at the time when $\eta \simeq \varepsilon \simeq 1$ is realized. For convenience, we will denote the field value at the end of inflation by subscript letter e, such as $\eta(\varphi_e) = \eta(\chi_e) = 1$ from now on.

Using the slow-roll parameters, observational cosmological parameters such as the scalar spectrum index n_s, the tensor-to-scalar perturbation ratio r and the the running of n_s can be represented as

$$n_s \simeq 1 - 6\varepsilon + 2\eta, \tag{4.26}$$

$$r \simeq 16\varepsilon, \tag{4.27}$$

$$n_s' := \frac{dn}{d\ln k} \simeq 16\varepsilon\eta - 24\varepsilon^2 - 2\xi. \tag{4.28}$$

The power spectra of curvature perturbations on the super-Hubble scales can be conveniently expanded as [17, 24, 73]

$$\mathcal{P}_{\mathcal{R}}(k) \simeq \Delta^2_{\mathcal{R}} \left(\frac{k}{k^*}\right)^{(n_s-1)+\frac{1}{2}\frac{dn_s}{d\ln k}\ln(\frac{k}{k^*})}, \quad \Delta^2_{\mathcal{R}} := \left.\frac{V}{24\pi^2 M_{\rm pl}^4 \varepsilon}\right|_{k^*} \tag{4.29}$$

where $\Delta^2_{\mathcal{R}}$ is the scalar power spectrum amplitude at $k_* = 0.005$ Mpc^{-1} which is given about $\ln(10^{10}\Delta^2_{\mathcal{R}}) = 3.094 \pm 0.034$ (68% CL, *Planck* TT, TE, EE+lowP combination data) [17]. The mode $k_* = a_* H_*$ represents the comoving wave number mode when it is crossing the Hubble radius for the first time. This number fixes the quantity of (V/ε) such as $r = 0.2$ with the BICEP2 result, the energy scale of inflation is $V \approx 7.19 \times 10^{-9} M_{\rm pl}^4$ at horizon exit. The equation (4.29) helps us to

determine c_1 parameter in the potential (4.6) as

$$c_1 = 24\pi^2\Delta^2_{\mathcal{R}}\left(\frac{\varphi_*}{\sqrt{2}M_{\rm pl}}\right)^{-2n}\left.\frac{\varepsilon}{A(\varphi_*)}\right|_{k_*}. \tag{4.30}$$

The e-folding number induced by changing of inflaton from χ at a particular scale to χ_e at the end of inflation can be written as

$$\begin{aligned} N &= -\frac{1}{M^2_{\rm pl}}\int_{\chi}^{\chi_e}\frac{V}{V'}d\chi = -\frac{1}{M^2_{\rm pl}}\int_{\varphi}^{\varphi_e}\frac{V}{V'}\left(\frac{d\chi}{d\varphi}\right)d\varphi \\ &= -\frac{1}{nm^2}\left(\frac{\Lambda}{M_{\rm pl}}\right)^{-4}\int_{\phi}^{\phi_e}\phi^5\left(\frac{1-2c_2\phi^{2m}}{n-2c_2(n+m)\phi^{2m}}\right)d\phi \\ &= -\frac{1}{nm^2}\left(\frac{\Lambda}{M_{\rm pl}}\right)^{-4}\int_{\phi}^{\phi_e}\left[\phi^5+\frac{2c_2m}{n}\frac{\phi^{2m+5}}{(1-2c_2(1+(m/n))\phi^{2m})}\right]d\phi. \end{aligned} \tag{4.31}$$

Here, we used notation in equation (4.5) to shorten the notation in the second and the third line. The fist integral is trivial. Hence we only need to focus on the second integral. One of crucial steps to solve analytically this term is to expand the binomial function in the denominator factor. It is possible to do as if $c_2 = \mathcal{O}(1), m < n$ and $\phi < 1$, and then the factor satisfies $|2c_2(1+(m/n))\phi^{2m}| < 1$.

The binomial function itself corresponds to Hyperbolic function [74, 75] by relation

$$(1-x)^{-\alpha} = {}_2F_1(\alpha,\beta,\beta;x) = {}_1F_0(\alpha;-;x) = \sum_{n=0}^{\infty}\frac{(\alpha)_n}{n!}x^n. \tag{4.32}$$

Notations ${}_2F_1(a,b;c;x)$ and ${}_1F_0(a;x)$ are particular cases for general Hyperbolic function given by

$${}_pF_q(a_1,\cdots,a_p;b_1,\cdots,b_q;x) := \sum_{n=0}^{\infty}\frac{(a_1)_n\cdots(a_p)_n}{(b_1)_n\cdots(b_q)_n n!}x^n \tag{4.33}$$

where $(w)_n := \frac{\Gamma(w+n)}{\Gamma(w)} = w(w+1)(w+2)\cdots(w+n-1)$, $(w)_0 = 1$ is a Pochhammer symbol. This series converges for all x if $p \leq q$, for $|x|< 1$ if $p = q+1$ and diverges for all $x \neq 0$ if $p > q+1$. Therefore, the second integral in the last line of equation (4.31) converges if the corresponding Hyperbolic function is ${}_{(q+1)}F_q$.

Denoting $2c_2(1+(m/n)) := \beta$, the second integral part in equation (4.31) can be expanded to be

$$\begin{aligned}\int \frac{\phi^{2m+5}}{(1-\beta\phi^{2m})^{\alpha}} d\phi &= \int \phi^{2m+5} \left(\sum_{j=0}^{\infty} \frac{(\alpha)_j}{j!} \left(\beta\phi^{2m}\right)^j \right) d\phi \\ &= \left(\sum_{j=0}^{\infty} \frac{(\alpha)_j}{[2m(j+1)+6]\, j!} \left(\beta\phi^{2m}\right)^j \right) \phi^{2m+6}. \end{aligned} \tag{4.34}$$

When $\alpha = 1$, factor $(\alpha)_j$ and $j!$ eliminate each other. Furthermore, by manipulation to the factor, we have the relation

$$\begin{aligned}\frac{1}{2m(j+1)+6} &= \frac{1}{6} \frac{\left(\frac{6}{2m}\right)\left(\frac{6}{2m}+1\right)\left(\frac{6}{2m}+2\right)\cdots\left(\frac{6}{2m}+j\right)}{\left(\frac{6}{2m}+1\right)\left(\frac{6}{2m}+2\right)\cdots\left(\frac{6}{2m}+j\right)\left(\frac{6}{2m}+(j+1)\right)} \\ &= \frac{1}{2(3+m)} \frac{\left(\frac{3}{m}+1\right)_j}{\left(\frac{3}{m}+2\right)_j}. \end{aligned} \tag{4.35}$$

As the result, equation (4.34) can be expressed as

$$\begin{aligned}\int \frac{\phi^{2m+5}}{(1-\beta\phi^{2m})^{\alpha}} d\phi &= \left(\frac{1}{2(3+m)} \sum_{j=0}^{\infty} \frac{(\alpha)_j \left(\frac{3}{m}+1\right)_j}{\left(\frac{3}{m}+2\right)_j\, j!} \left(\beta\phi^{2m}\right)^j \right) \phi^{2m+6} \\ &= \frac{\phi^{2m+6}}{2(3+m)}\ {}_2F_1\left(\alpha, \frac{3}{m}+1; \frac{3}{m}+2; \beta\phi^{2m}\right). \end{aligned} \tag{4.36}$$

Collecting everything in one peace, we can rewrite the e-folding number in an expression

$$N := N(\varphi) - N(\varphi_e) \tag{4.37}$$

where $N(\varphi)$ is defined as

$$\begin{aligned} N(\varphi) := \frac{1}{6nm^2} \left(\frac{\Lambda}{M_{\rm pl}}\right)^{-4} \left(\frac{\varphi}{\sqrt{2}M_{\rm pl}}\right)^6 \Bigg[1 + \frac{6c_2 m}{n(3+m)} \left(\frac{\varphi}{\sqrt{2}M_{\rm pl}}\right)^{2m} \\ \times\ {}_2F_1\left(1, \frac{3}{m}+1; \frac{3}{m}+2; 2c_2\left(1+\frac{m}{n}\right)\left(\frac{\varphi}{\sqrt{2}M_{\rm pl}}\right)^{2m}\right)\Bigg]. \end{aligned} \tag{4.38}$$

In many cases such as $n = 3$ and $m = 1$, the expression of $N(\chi)$ might be approximately given by the first terms since the bracket terms tend to be much smaller by factor $\phi^{2m}\ {}_2F_1(1, a; a+1; \beta\phi^{2m})$. Even in that case, the value of e-folding in the end of inflation $N(\chi_e)$ could not be neglected because χ_e is not small enough compared to χ in sufficiently realized inflation. We will show in the next discussion how the inflation ends even before the condition $\varepsilon(\varphi_e) \simeq 1$ is reached. On the other hand, to produce sufficient inflation, e-folding number N at horizon crossing is usually taken in the range $50 - 60$ to accommodate uncertainty in the various energy scales connected with inflation in the model [76, 77]. We denote it as N_* and the corresponding field value as φ_*. Practically, all of the slow-roll parameters and cosmological parameters associated to the observations should be represented at the k_* scale.

4.3 Inflaton dynamics

To understand whole processes that the scalar field S will undergo, it is useful to investigate the time evolution of the fields. Each component field $\varphi_{1,2}$ of the scalar field $S = \frac{1}{\sqrt{2}}(\varphi_1 + i\varphi_2)$ follows the equation of motions as follows:

$$\ddot{\varphi}_i + 3H\dot{\varphi}_i = -\frac{\partial V}{\partial \varphi_i} \quad (i = 1, 2), \tag{4.39}$$

where the Hubble parameter H of the system is now written as $H^2 = \frac{1}{3M_{\rm pl}^2}\left(\sum_i \frac{1}{2}\dot{\varphi}_i + V\right)$ and $\frac{\partial V}{\partial \varphi_i}$ denotes the partial derivative of potential $V(S)$ in the direction of the field

component φ_i. For any number of n and m, $\frac{\partial V}{\partial \varphi_i}$ can be expressed respectively as

$$\begin{aligned}\frac{\partial V}{\partial \varphi_1} = \frac{c_1}{M_{\rm pl}^{2n-4}}\left(S^\dagger S\right)^n \Bigg[& \frac{n\varphi_1}{(S^\dagger S)} \\ & + \frac{c_2}{M_{\rm pl}^{2m}}\left\{\frac{n\varphi_1\left(S^{2m}+(S^\dagger)^{2m}\right)}{(S^\dagger S)} + \frac{2m\left(S^{2m-1}+(S^\dagger)^{2m-1}\right)}{\sqrt{2}} + \frac{i\varphi_1\left(S^{2m}-(S^\dagger)^{2m}\right)}{\Lambda^2}\right\} \\ & \qquad \times \cos\left(\frac{iS^\dagger S}{\Lambda^2}\right) \\ & + \frac{c_2}{M_{\rm pl}^{2m}}\left\{\frac{n\varphi_1\left(S^{2m}-(S^\dagger)^{2m}\right)}{(S^\dagger S)} + \frac{2m\left(S^{2m-1}-(S^\dagger)^{2m-1}\right)}{\sqrt{2}} + \frac{i\varphi_1\left(S^{2m}+(S^\dagger)^{2m}\right)}{\Lambda^2}\right\} \\ & \qquad \times \sin\left(\frac{iS^\dagger S}{\Lambda^2}\right)\Bigg], \end{aligned} \tag{4.40}$$

and

$$\begin{aligned}\frac{\partial V}{\partial \varphi_2} = \frac{c_1}{M_{\rm pl}^{2n-4}}\left(S^\dagger S\right)^n \Bigg[& \frac{n\varphi_2}{(S^\dagger S)} \\ & + \frac{c_2}{M_{\rm pl}^{2m}}\left\{\frac{n\varphi_2\left(S^{2m}+(S^\dagger)^{2m}\right)}{(S^\dagger S)} + \frac{2mi\left(S^{2m-1}-(S^\dagger)^{2m-1}\right)}{\sqrt{2}} + \frac{i\varphi_2\left(S^{2m}-(S^\dagger)^{2m}\right)}{\Lambda^2}\right\} \\ & \qquad \times \cos\left(\frac{iS^\dagger S}{\Lambda^2}\right) \\ & + \frac{c_2}{M_{\rm pl}^{2m}}\left\{\frac{n\varphi_2\left(S^{2m}-(S^\dagger)^{2m}\right)}{(S^\dagger S)} + \frac{2mi\left(S^{2m-1}+(S^\dagger)^{2m-1}\right)}{\sqrt{2}} + \frac{i\varphi_2\left(S^{2m}+(S^\dagger)^{2m}\right)}{\Lambda^2}\right\} \\ & \qquad \times \sin\left(\frac{iS^\dagger S}{\Lambda^2}\right)\Bigg]. \end{aligned} \tag{4.41}$$

Taking a particular case with $m = 1$, those above equation can be simplified to be

$$\begin{aligned}\frac{\partial V}{\partial \varphi_1} = \frac{c_1\left(S^\dagger S\right)^n}{M_{\rm pl}^{2n-4}}\Bigg[& \frac{n\varphi_1}{(S^\dagger S)} + \frac{c_2\varphi_1}{M_{\rm pl}^2}\left\{\frac{n\left(\varphi_1^2-\varphi_2^2\right)}{(S^\dagger S)} + 2 - \frac{2\varphi_1\varphi_2}{\Lambda^2}\right\}\cos\left(\frac{S^\dagger S}{\Lambda^2}\right) \\ & - \frac{c_2\varphi_1}{M_{\rm pl}^2}\left\{\frac{2n\varphi_1\varphi_2}{(S^\dagger S)} + 2\frac{\varphi_2}{\varphi_1} + \frac{\left(\varphi_1^2-\varphi_2^2\right)}{\Lambda^2}\right\}\sin\left(\frac{S^\dagger S}{\Lambda^2}\right)\Bigg], \end{aligned} \tag{4.42}$$

$$\frac{\partial V}{\partial \varphi_2} = \frac{c_1 \left(S^\dagger S\right)^n}{M_{\rm pl}^{2n-4}} \left[\frac{n\varphi_2}{(S^\dagger S)} + \frac{c_2\varphi_2}{M_{\rm pl}^2} \left\{ \frac{n\left(\varphi_1^2 - \varphi_2^2\right)}{(S^\dagger S)} - 2 - \frac{2\varphi_1\varphi_2}{\Lambda^2} \right\} \cos\left(\frac{S^\dagger S}{\Lambda^2}\right) \right.$$
$$\left. - \frac{c_2\varphi_2}{M_{\rm pl}^2} \left\{ \frac{2n\varphi_1\varphi_2}{(S^\dagger S)} + 2\frac{\varphi_1}{\varphi_2} + \frac{(\varphi_1^2 - \varphi_2^2)}{\Lambda^2} \right\} \sin\left(\frac{S^\dagger S}{\Lambda^2}\right) \right]. \tag{4.43}$$

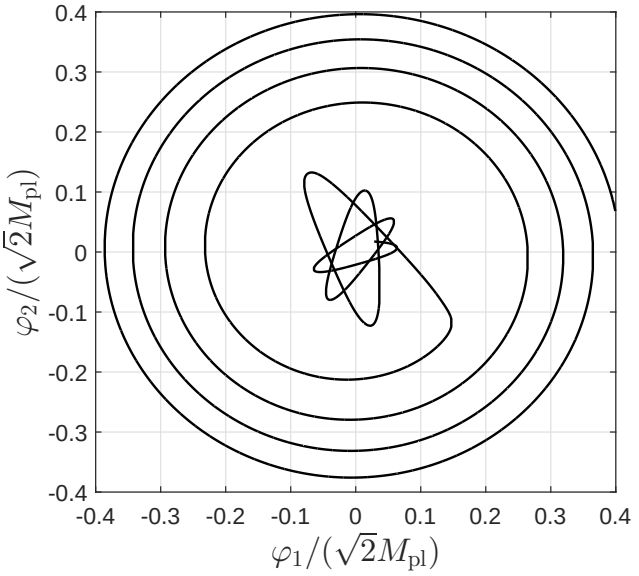

FIGURE 4.2: Inflaton dynamics for the $n = 2, m = 1$ case. Other parameters are fixed as the ones given in the caption of the Figure 4.1. The initial value of inflaton is fixed at a potential minimum.

Solving the above equations of motion numerically, the inflaton dynamics and the inflaton evolution are presented in the Figures 4.2 and 4.3. The initial value of the field could not be selected arbitrarily as it could ruin its dynamics depending on it. If the initial point of the inflation is located at (φ, θ) in the polar coordinate $\varphi^2 = \varphi_1^2 + \varphi_2^2$ and $\theta = \arctan(\varphi_1/\varphi_2)$ where $V_a(\varphi, \theta) > V_{max}$ is satisfied for the nearest local maximum V_{max}, the kinetic energy of the inflaton could be larger than the next potential hill when the inflaton reaches there. As the result, the inflaton could cross over the hill without realizing the slow-roll motion along the angular direction. The best way is to place the inflaton initial value at potential minimum.

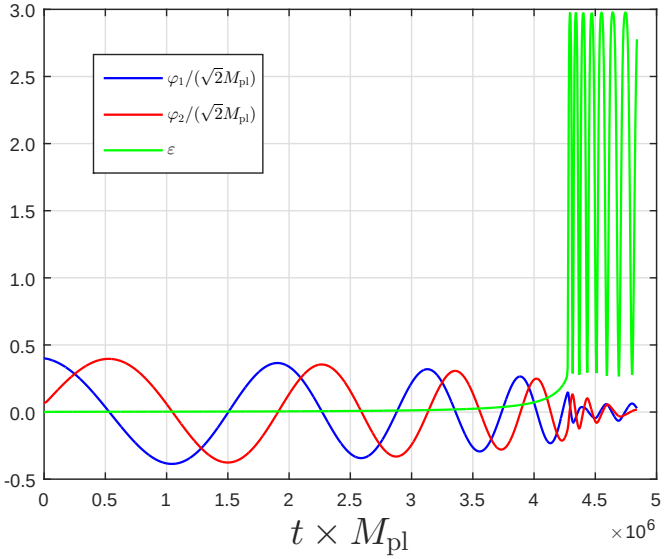

FIGURE 4.3: Inflaton evolution corresponds to the fields dynamics given in the Figure 4.2. Here $\varepsilon(t)$ is given. It shows how $\varepsilon(t)$ changes dramatically much before $\varepsilon = 1$ to stop the inflation period.

At a particular point, the motion suddenly falls toward of the center of the potential and starts the oscillation as illustrated in the Figure 4.2. This point is considered to the time when the inflation end and it is related to the time when $\varepsilon(t)$ is close to unity but mostly much less than unity. The time dependence of ε is illustrated in the Figure 4.3 to show how ε is dramatically changing near the turning point in the Figure 4.2. This turning point can be easily figured out in the Figure 4.3 as the time when the damping of the fields evolution starts. It is characterized by the rapid decrease of the amplitude and the frequency of the fields. Since the kinetic energy of the fields becomes larger compared with the local potential barrier which gradually becomes smaller, the field components are expected to leave the local minimum and go over the potential toward the global minimum at a certain period, at least when its kinetic energy is equal to the potential barrier $\dot{\chi}^2/2 \simeq V_b$. If we apply the slow-roll approximation $3H\dot{\chi} = -V'$, this period is given at $\varepsilon = \frac{3V_b(V_b+V)}{V^2}$. It is translated to

$$\frac{\varphi_e}{\sqrt{2}M_{\rm pl}} \simeq \left(\frac{m^2 n}{6c_2}\right)^{\frac{1}{2m+6}} \left(\frac{\Lambda}{M_{\rm pl}}\right)^{\frac{2}{m+3}}, \tag{4.44}$$

when the c_2 term contribution is neglected. In that case, the contribution of the e-folding number at the end of inflation $N(\chi_e)$ to the total e-folding number N could become significant. To confirm this behavior and to determine χ_e, we estimate it by using the numerical calculation so that the effect of the c_2 term can be fully understood.

4.4 Inflation parameters and its comparison with chaotic inflation

When the terms containing c_2 are negligible safely, the situation becomes much simple. The effective potential given in (4.7) has similar form with the power-law type chaotic inflation. Therefore, the features of are also similar. We list some inflation parameters for the inflation in comparison with the power-law chaotic inflation in the table 4.1 [70, 78].

$V(\varphi)$	ε	η	ξ	r	n_s	n_s'
$V_{\rm ch}$	$\frac{p}{4N_*}$	$\frac{p-1}{2N_*}$	$\frac{(p-1)(p-2)}{4N_*^2}$	$\frac{4p}{N_*}$	$1-\frac{p+2}{2N_*}$	$-\frac{(2+p)}{2N_*^2}$
$V_{\rm appx}$	$\frac{n}{6(N_*+N_e)}$	$\frac{2n-3}{6(N_*+N_e)}$	$\frac{(2n-3)(2n-6)}{6^2(N_*+N_e)^2}$	$\frac{8n}{3(N_*+N_e)}$	$1-\frac{n+3}{3(N_*+N_e)}$	$-\frac{(3+n)}{3(N_*+N_e)^2}$

TABLE 4.1: Comparison table between power-law chaotic inflation with a potential $V_{\rm ch}=\alpha^4\left(\frac{\varphi}{M_{\rm pl}}\right)^p$ and the c_2 terms negligible limit in our model with the approximated potential $V_{\rm appx}=c_1M_{\rm pl}^4\left(\frac{\varphi}{\sqrt{2}M_{\rm pl}}\right)^{2n}$.

The m dependency is explicitly contained in the e-folding (N_*+N_e) even though it does not appear in these approximated formulas. There are some interesting features in this limit compared to the power-law chaotic inflation. The first one is the correspondence between two models appears for $p=2n/3$. the next one is that the e-folding number at the horizon exit N_* in the power-law chaotic inflation corresponds to (N_*+N_e). The N_* is the e-folding number at the horizon exit and known have favorable value about 50-60 to produce the sufficient inflation and $N_e=N(\chi_e)$ is the e-folding number at the end of inflation stage which might not be negligible in the present model. As the result, the parameters such as the tensor-to-scalar ratio r tends to be smaller and the spectral index n_s tends to be higher

then those in the chaotic inflation, respectively. The last one is the absolute value of the running of the spectral index n_s' tends to be smaller than that in the chaotic inflation for all n value even if N_e have been included. Planck 2015 confirmed a smaller tensor-to-scalar ratio and smaller absolute value of running of the spectral index and a larger spectral index compared to those in BICEP2 [17, 79]. Therefore, even thought the power-law chaotic inflation with $p \geq 2$ has been disfavored by Planck 2015 at $\geq 3\sigma$, the present model could survive even for the negligible c_2 limit. We will show later how $n = 3$ which corresponds to $p = 2$ could be within 2σ region after including c_2 terms.

By using relation between scalar power spectrum $\Delta^2_{\mathcal{R}}$ in the equation (4.29), the potential (4.7) and the slow-roll parameter ε given in the table 4.1, the parameter c_1 can be approximately written in the limit of negligible c_2 as

$$c_1 = 9.5 \times 10^{-8} \frac{n}{N_* + N_e} \left(\frac{\varphi_*}{\sqrt{2} M_{\rm pl}} \right)^{-2n} . \tag{4.45}$$

For the example, taking $n = 3$ and $N_* + N_e = 60$, we have $c_1 \simeq 1.159 \times 10^{-6}$ for $\left(\frac{\varphi_*}{\sqrt{2}M_{\rm pl}}\right) = 0.40$. This approximation is still valid even for $c_2 = \mathcal{O}(1)$. As we can see, if c_1 is rescaled to $x^{2n}c_1$ by a factor x (> 0), the potential form in the equation (4.1) can be kept invariant by rescaling the other parameters: as $c_2 \mapsto x^{2m}c_2, \Lambda \mapsto x^{-1}\Lambda$ and $\varphi_* \mapsto x^{-1}\varphi_*$. Consequently, larger c_2, smaller Λ and smaller φ_* are needed to compensate a larger c_1 value. Otherwise, to compensate a larger c_2 value, the larger c_1 , the smaller Λ and smaller φ_* are required. Even though the effect of changing the c_2 value might not be clearly recognized from the equation (4.45), this property explains the basic features of this model which are represented in the computational results shown in the next section.

4.5 Constraints from Planck 2013, Bicep2 and Planck 2015

The Planck 2013, combined with the WMAP large-angle, constrains the scalar spectral index to be $n_s = 0.9603 \pm 0.0073$ and the scalar power spectrum amplitude

to be $\Delta^2_{\mathcal{R}} = 2.196^{+0.051}_{-0.06} \times 10^{-9}$. It also and establishes an upper bound on the tensor-to-scalar ratio as $r < 0.11$ (95% CL) at the pivot scale $k_* = 0.002$ Mpc^{-1}. An important point of this result is that the scale invariance is confirmed at over 5σ level. Thus, any models predicting subtantial deviation from the nearly scale invariance and a blue tilted scalar power spectrum, such as a original hybrid model, are ruled out. Moreover, the level of local non-Gaussianities is constrained by a bound $f^{\rm loc}_{\rm NL} = 2.7 \pm 5.8$ that disfavors exotic and complicated dynamical possibilities, such as inflationary models with non-canonical kinetic energy and multiple fields. Planck 2013 data thus prefers single field inflation to more complicated possibilities. Some of them, i.e. exponential potential models, the simplest hybrid inflationary models, and monomial potential models of degree $n \geq 2$, do not provide a good fit to the data [14]. However, Bicep2 measures rather higher tensor-to-scalar ratio than that measured by Planck 2013. The bound is given at $r = 0.20^{+0.07}_{-0.05}$ without dust foreground subtraction that disfavors $r = 0$ at 7.0σ level, or it is given at $r = 0.16^{+0.06}_{-0.05}$ if dust foreground subtraction is included [72, 80]. Monomial potential with power $2 \leq p \leq 3$ survives under this new constrain [70]. It has been mentioned in the previous section that the behavior of this inflationary model would be similar and comparable to it since the leading contribution of the scalar potential responsible to the inflation takes form of a power-law potential. The existence of c_2 term in our model leads to better predictions than that in the ordinary monomial chaotic inflation. Here we give more attention to $p = 2$ which corresponds to $n = 3$ in our model to minimize the tension between the results of Planck 2013 and Bicep2. Predictions given for some parameter sets for $n = 3$ and $m = 1$ are presented in the Table 4.2 and in the Figure 4.4.

	c_1	c_2	$\frac{\Lambda}{M_{\rm pl}}$	$\frac{\varphi^*}{\sqrt{2}M_{\rm pl}}$	H^*(GeV) $\times 10^{14}$	N^*	n_s	r	n'_s
A	1.66×10^{-6}	0.7	0.04	0.378	0.871	59.0	0.971	0.107	-0.00016
	2.04×10^{-6}	0.7	0.04	0.371	0.921	54.2	0.968	0.119	-0.00022
	2.42×10^{-6}	0.7	0.04	0.366	0.965	49.1	0.965	0.131	-0.00027
B	0.257	6.0	0.002	0.0512	0.945	60.4	0.969	0.124	-0.00046
	0.305	6.0	0.002	0.0505	0.986	55.0	0.966	0.136	-0.00054
	0.364	6.0	0.002	0.0498	1.030	50.0	0.962	0.149	-0.00064

TABLE 4.2: Predictions for some typical parameter sets of the model defined for $n = 3$ and $m = 1$.

The predictions given in the Table 4.2 are fully generated by using numerical calculation to get solutions of the field evolution equation (4.39). Local minimum of the potential is applied as the initial point of inflation to get an appropriate dynamics and thenthe inflation stops at the point where the inflaton starts falling to the global minimum. As we can estimate the e-folding number by equation (4.31) along the trajectory of inflaton, φ_* can be decided by $N_* = N(\varphi_*) - N(\varphi_e)$. Here the field value at the end of inflation is denotes as φ_e and we take $N_* = 50 - 60$ which is required to generate sufficient inflation stage. H^* is the Hubble parameter calculated at φ_* and is proportional to the energy scale during inflation. Other variables related to the inflation variables, i.e. the tensor-to-scalar ratio r, the spectral index n_s and the running n_s' are also estimated at φ_* as well.

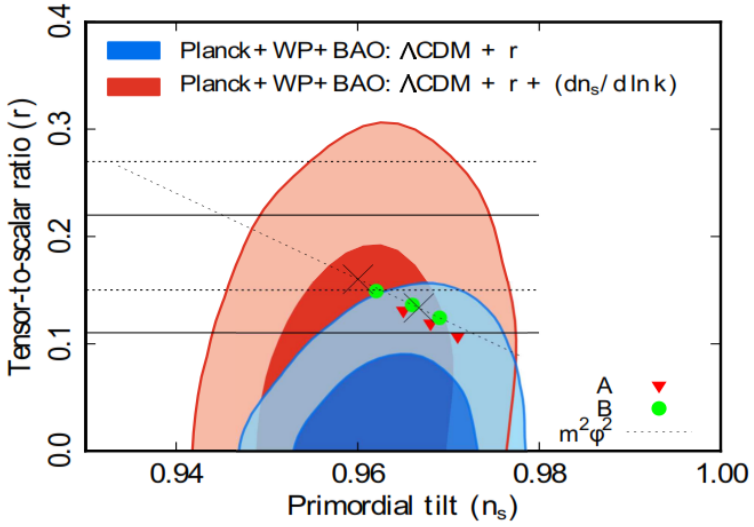

FIGURE 4.4: Predicted values of (n_s, r) for several parameter sets $\left(c_2, \frac{\Lambda}{M_{\rm pl}}\right)$ given in the Table 4.2 are plotted here. The dotted line represents the prediction of the quadratic chaotic inflation model, in which the points corresponding to $N_* = 50$ and 60 are represented as crossed lines. The horizontal solid lines and dotted lines represent the Bicep2 1σ constraints with and without the foreground subtraction, respectively [72]. The contours given as Figure 4 in Planck Collaboration XXII [14] are used here. Since the running of the spectral index is negligible, the blue contour should be compared with the predictions

Table 4.2 shows that sufficiently large N_* can be realized as long as $\Lambda \ll \varphi_*$ is satisfied, even for sub-Planckian value $\varphi_* < M_{\rm pl}$. The Hubble parameter during inflation takes the value around 10^{14} GeV as shown in the Table. It should be noted

that r and n_s favored by the present constraints could be possibly achieved by the parameters c_2 and Λ in rather width ranges in this model. The predicted r and n_s are then plotted in the Figure 4.4 using contours provided by Planck Collaboration XXII [14]. To present Bicep2 constraint on the tensor-to-scalar ratio, the bounds are displayed as horizontal lines in the contours. Here we take the contours that are suitable for negligible running of the spectral index as they were predicted too small in this model. As a comparison, predictions given by quadratic chaotic inflation are shown in the figure.

The Figure 4.4 shows that the predictions are somehow shifted from the quadratic chaotic inflation prediction. Both $N_* = 50$ and 60 tend to predict larger spectral index value and smaller tensor-to-scalar ratio value than those of the quadratic chaotic inflation. These can be understood from the fact that this model predicts smaller ε and larger η affected by the presence of the c_2 term. Even for negligible c_2 terms, since $N(\varphi_e)$ has a significant contribution to the e-folding during inflation as already explained in the previous section, r and n_s are predicted smaller and larger than those in the quadratic chaotic inflation.

n	c_1	c_2	$\frac{\Lambda}{M_{\rm pl}}$	$\frac{\varphi_1^*}{\sqrt{2}M_{\rm pl}}$	H_* ($\times 10^{13}$GeV)	N_*	n_s	r	n_s'
3	1.00×10^{-6}	1.5	0.05	0.417	6.528	60.0	0.967	0.070	-0.00047
	9.84×10^{-7}	1.7	0.05	0.411	5.914	60.0	0.964	0.056	-0.00043
	8.62×10^{-7}	1.9	0.05	0.406	5.399	60.0	0.959	0.040	-0.00032
2	1.32×10^{-7}	1.1	0.05	0.394	7.019	60.0	0.973	0.058	-0.00043
	1.76×10^{-7}	1.1	0.05	0.384	6.725	50.0	0.968	0.072	-0.00061
	1.22×10^{-7}	1.6	0.05	0.383	5.931	60.0	0.969	0.039	-0.00040
	1.71×10^{-7}	1.6	0.05	0.374	5.767	50.0	0.964	0.052	-0.00059
	1.03×10^{-7}	1.9	0.05	0.374	5.318	60.0	0.963	0.026	-0.00035
1	1.36×10^{-8}	0.5	0.05	0.349	5.079	50.0	0.975	0.041	-0.00046
	7.45×10^{-9}	1.6	0.05	0.333	4.146	60.0	0.970	0.015	-0.00036
	1.02×10^{-9}	1.6	0.05	0.326	4.102	50.0	0.966	0.019	-0.00052
	6.15×10^{-9}	1.8	0.05	0.327	3.976	60.0	0.966	0.011	-0.00035
	8.77×10^{-9}	1.8	0.05	0.320	3.944	50.0	0.962	0.016	-0.00052

TABLE 4.3: Examples of the predicted values for the spectral index n_s and the tensor-to-scalar ratio r in this scenario with $m = 1$.

To complete the discussion, the constraints given by Planck 2015 might be included. The Planck 2015 mission releases the announcement that the spectral index of curvature perturbations is measured to be $n_s = 0.968 \pm 0.006$ with the tight constraint of scale dependence $dn_s/d\ln k = ? 0.003 \pm 0.007$. The upper bound on the tensor-to-scalar ratio is $r < 0.11(95\%\ \mathrm{CL})$ measured at pivot scale $k_* = 0.002\ \mathrm{Mpc}^{-1}$ which is consistent with the B-mode polarization constraint $r < 0.12(95\%\ \mathrm{CL})$ measured at $k_* = 0.05\mathrm{Mpc}^{-1}$ obtained from a joint analysis of the BICEP2/Keck Array and Planck data. One of the implication of these bounds is that the inflation with quadratic potential and natural inflation are now completely disfavored. A stronger constraint is given by a smaller tensor-to-scalar ratio measured by Planck 2015 than before. Even so, monomial inflation with power $p < 2$ is found to survive from the constraint [17]. Due to this finding, we need to consider new parameter sets given for $n \leq 3$ to find new predictions in this model. The examples of predicted results are shown in the Table 4.3 and the complete predictions are plotted in the Figure 4.5.

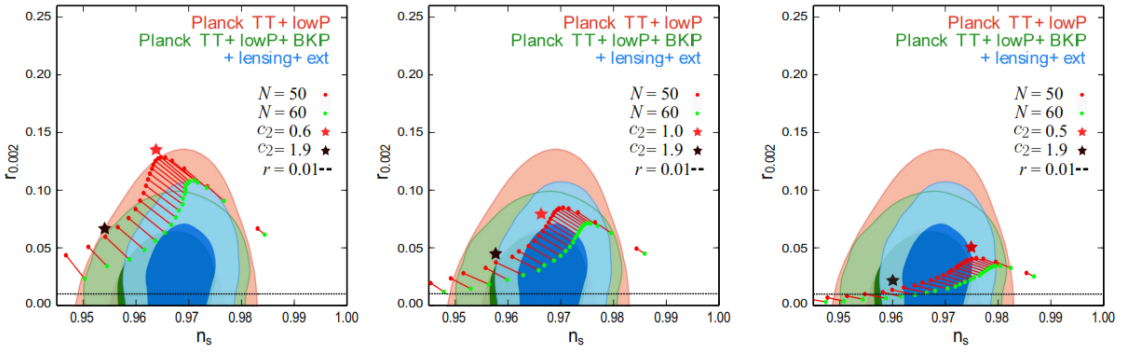

FIGURE 4.5: Predicted regions in the (n_s, r) plane are presented in panel (a) for $n = 3$, in panel (b) for $n = 2$, and in panel (c) for $n = 1$. Λ is fixed as $\Lambda = 0.05 M_{\mathrm{pl}}$ in all cases. The values of c_1 and φ_* are given in Table 4.3 for representative values of c_2. Contours given in the right panel of Fig. 21 in Planck 2015 results.XIII.[81] are used here. Horizontal black lines $r = 0.01$ represent a possible limit detected by LiteBIRD in near future.

Table 4.3 shows numerical examples for the cases $n = 1, 2, 3$ with a fixed Λ. In such cases, the first term in the potential differs from each other. For $n = 1$, the

first term of the potential is $c_1 M_{\rm pl}^2 S^\dagger S$ which coincides with $\tilde{m}_S^2 S^\dagger S$ and for $n = 2$ is given by $c_1 (S^\dagger S)^2$ which coincides with $\kappa_1 (S^\dagger S)^2$. Due to the assumption that the inflaton potential is dominant during inflation stage, those terms are assumed to be prominent compared with others in each case. The values of c_1 and φ_* are fixed by the normalization condition given in the equation (4.29) for each value of c_2. The predicted points are plotted in the (n_s, r) plane with the contours taken from the right panel of Fig. 21 in Planck 2015 results.XIII.[81] as again the predicted value of the running of the spectral index is negligible in this model. The red and green circles displayed in figure correspond to $N_* = 50$ and 60, respectively. The predictions are plotted for every 0.1 of c_2 starting from $c_2 = 0.1$ on the right-hand side while Λ is fixed as $\Lambda = 0.05 M_{\rm pl}$. We show the boundary values of c_2 by the red and black stars, for which either red or green circles are inside of the region of 2σ CL and 1σ CL of the latest Planck TT+lowP+ BKP+lensing+ext combined data for the $n = 3$ and $n = 1, 2$ panels, respectively. The predictions within those interval are favored by the latest Planck data combined with others. The best fit result is obtained for the $n = 1$ case. Here, the bound for future CMB detection, LITEBIRD as an example that is expected to detect the signal of the gravitational wave with $r > 0.01$ at more than 10σ [82], is given in the figure.

4.6 Reheating after inflation

Reheating at the end of the inflation period is an important part of the inflation scenario. At this stage, inflaton energy is transferred to the radiation energy and reheat the universe after inflation. In terms of equation of motion of the inflaton field, there is an additional damping term due to the energy loss caused by the particle production from the inflaton decay besides the energy loss due to the universe expansion. There is a time that the Hubble parameter decrease to a value comparable with the decay rate of inflaton. The particle production due to the inflaton decay becomes effective at such a time. This reheating stage after inflation corresponds to a certain period when inflaton starts to behave as matter through the oscillation around the global minimum of the potential.

The early stage of the reheating may be constituted by two main processes: preheating due to the parametric resonance through quartic interactions of S with Φ and η and the perturbative decay due to an interaction term $\mu S\eta^\dagger\Phi$. The first constituent may not occur effectively as the fields coupled to $\varphi_{1,2}$ have large effective mass so it seems difficult for $\varphi_{1,2}$ to produce these particles. The perturbative decay due to $\frac{\mu}{\sqrt{2}}\varphi_1\eta^\dagger\Phi$ and $\frac{i\mu}{\sqrt{2}}\varphi_2\eta^\dagger\Phi$ takes place to complete energy transfer from the inflaton to the radiation. The decay width of each process is given by $\Gamma_{\varphi_i} = \frac{1}{8\pi}\frac{|\mu|^2}{\bar{m}_i}$ where $\bar{m}_1^2 = \tilde{m}_S^2 + m_S^2$ and $\bar{m}_2^2 = \tilde{m}_S^2 - m_S^2$ are the mass of φ_1 and φ_2, respectively. As $\tilde{m}_S$ is assumed much larger than m_S, the reheating temperature given from this perturbative decay can be estimated as [83–85]

$$T_R \simeq 0.35 g_*^{-1/4} |\mu| \sqrt{\frac{M_{\rm pl}}{\tilde{m}_S}}, \tag{4.46}$$

where here $g_* = 116$ denotes the relativistic degree of freedom chosen in this model. To estimate this temperature, μ and $\tilde{m}_S$ need to be given qualitatively. These quantities can be constrained by the neutrino mass generation through equation (3.25) and condition on the mass of φ during inflation given in the equation (4.9). As potential (4.1) is assumed to dominate the potential during inflation, we have a condition $\tilde{m}_S \ll m_\varphi$ or

$$\tilde{m}_S \ll \sqrt{c_1}\left(\frac{\varphi_*}{M_{\rm pl}}\right)^{n-2}\varphi_* \tag{4.47}$$

$$\simeq 3.1\times 10^{-4}\left(\frac{n}{N_*}\right)^{1/2}\left(\frac{M_{\rm pl}}{\varphi_*}\right)^2\varphi_*, \tag{4.48}$$

This constraint on $\tilde{m}_S$ now depends on the typical n taken in the calculation. Taking $n = 3$, $\varphi_* \simeq 0.5 M_{\rm pl}$ and $N_* = 60$ as an example it gives the bound $\tilde{m}_S \ll 3.4\times 10^{14}$ GeV. As the result, the reheating temperature can be estimated as

$$T_R \simeq 1.6\times 10^8 \left(\frac{|\lambda_5|}{10^{-6}}\right)^{1/2}\left(\frac{\tilde{m}_S}{m_S}\right)\sqrt{\frac{\tilde{m}_S}{10^6\ \text{GeV}}}\quad \text{GeV}. \tag{4.49}$$

If we taking the lightest neutral component of η as dark matter with mass of order 1 TeV, it suggests that $|\lambda_5|$ should be $O(10^{-6})$ or less [86, 87]. Thus the reheating temperature would be vary in the range of 10^5 GeV $\leq T_R \leq 10^{15}$ GeV depending

on the value of $\tilde{m}_S$. This order is high enough to produce termal right-handed neutrinos of $O(1)$ TeV to produce sufficient baryon asymmetry via leptogenesis.

Chapter 5

Summary

An extension of the radiative neutrino masses model by a complex singlet has been considered to explain the inflation of the universe by keeping favorable features of the original model, the simultaneous explanation of the small neutrino masses, the DM abundance and the baryon number asymmetry in the Universe. The complex singlet not only plays a role in the inflation scenario due to its component but is also involved in the neutrino mass generation at one loop to explain the smallness of neutrino masses. By choosing a complex scalar potential that realizes a dynamics of the inflaton following a spiral-like valley, trans-Planckian field variation can be realized to generate the sufficient e-foldings even though the relevant field is kept sub-Planckian. The η problem is now stated in the different way, that is the mass hierarchy of $\tilde{m}_S^2, m_S^2, \kappa\varphi^2 \ll H^2$ which is relevant to the neutrino mass and the scale hierarchy $\Lambda \ll M_{\rm pl}$ which is closely related to the UV completion theory of the present model. Therefore the η problem is still remaining in this model. The UV completion of the model is expected to give a solution for it. The origin of the potential cannot be still discovered at this stage.

The model interestingly behaves like a single field inflation scenario which is closely related with the power-low chaotic inflation in a limiting case. Therefore, to make the predictions coincide with the present CMB results, we have mainly elaborated the corresponding parameters to the favorable power-law chaotic inflation. We have given the predictions by solving numerically the field equations for the

component fields of the singlet scalar for more general cases. The spectral index n_s and the tensor-to-scalar ratio r predicted by this model could have favorable values from the recent CMB observations by choosing the parameter sets in the inflaton potential. We have shown that the predicted values for them by using the parameter sets for $n = 1, 2$ and $m = 1$ are favorable even for Planck 2015 observational constraints.

Furthermore, the rough estimation of the reheating temperature in this model could be high enough to produce thermal right-handed neutrinos for resonant leptogenesis. Therefore, the model seems to have no serious difficulty to explain the crucial problems beyond the SM including the baryon number asymmetry like the original model of the radiative neutrino masses model.

Bibliography

[1] Fukuda, Y. et al. [Super-Kamiokande Collaboration] , Evidence for oscillation of atmospheric neutrinos, Phys.Rev.Lett. 81 (1998) 1562-1567.

[2] Ahn, M.H. et al. [K2K Collaboration], Indications of neutrino oscillation in a 250 km long baseline experiment, Phys.Rev.Lett. 90 (2003) 041801.

[3] Abe, K. et al. [T2K Collaboration], Indication of Electron Neutrino Appearance from an Accelerator-produced Off-axis Muon Neutrino Beam, Phys.Rev.Lett. 107 (2011) 041801.

[4] An, F.P. et al. [DAYA-BAY Collaboration], Observation of electron-antineutrino disappearance at Daya Bay, Phys.Rev.Lett. 108 (2012) 171803.

[5] Julian, William H, On the Effect of Interstellar Material on Stellar Non-Circular Velocities in Disk Galaxies, Astrophys.J. 148 (1967) 175.

[6] Tegmark, Max et al. [SDSS Collaboration], Cosmological parameters from SDSS and WMAP, Phys.Rev. D69 (2004) 103501.

[7] Riotto, Antonio et al, Recent progress in baryogenesis, Ann.Rev.Nucl.Part.Sci. 49 (1999) 35-75 .

[8] Dine, Michael et al, The Origin of the matter-antimatter asymmetry, Rev.Mod.Phys. 76 (2003) 1.

[9] Barbieri, Riccardo et al, Improved naturalness with a heavy Higgs: An Alternative road to LHC physics, Phys.Rev. D74 (2006) 015007.

[10] Ernest Ma, Common Origin of Neutrino Mass, Dark Matter, and Baryogenesis, Mod.Phys.Lett. A21 (2006) 1777-1782, arXiv:hep-ph/0605180.

[11] T. Hambye, F.-S. Ling, L. Lopez Honorez, and J. Rocher, Scalar Multiplet Dark Matter, JHEP 1005 (2010) 066, arXiv:0903.4010 [hep-ph].

[12] Daijiro Suematsu, Extension of a radiative neutrino mass model based on a cosmological view point, Phys.Rev. D85 (2012) 073008.

[13] Shoichi Kashiwase and Daijiro Suematsu, Leptogenesis and dark matter detection in a TeV scale neutrino mass model with inverted mass hierarchy, Eur.Phys.J. C73 (2013) 2484.

[14] P. Ade et al., Planck 2013 results. XXII. Constraints on inflation, arXiv:1303.5082 [astro-ph.CO], 2013.

[15] P. A. R. Ade et al. [BICEP2 Collaboration], arXiv:1403.4302 [astro-ph.CO].

[16] David H. Lyth, What would we learn by detecting a gravitational wave signal in the cosmic microwave background anisotropy?, Phys.Rev.Lett. 78 (1997) 1861-1863.

[17] P. A. R. Ade et al., Planck 2015 results. XX. Constraints on inflation, arXiv:1502.02114v1 [astro-ph.CO].

[18] Lerner, Rose N. et al, Distinguishing Higgs inflation and its variants, Phys.Rev. D83 (2011) 123522.

[19] Lerner, Rose N. et al., Unitarity-Violation in Generalized Higgs Inflation Models, JCAP 1211 (2012) 019.

[20] Junichi Yokoyama, Inflation: $1980 - 201X$, Prog. Theor. Exp. Phys. 2014, 06B103.

[21] Alan H. Guth, The Inflationary Universe: A Possible Solution to the Horizon and Flatness Problems, Phys.Rev. D23 (1981) 347-356.

[22] Guth, A., and P. J. Steinhardt (1984). Sci. Am. 250 (No. 5), 116.

[23] P. D. B. Collins, A. D. Martin and E. J. Squires, 1989, Particle physics and cosmology, A Wiley-Interscience Publ.

[24] P. Ade et al., Planck 2013 results. XVI. Cosmological parameters, arXiv:1303.5076 [astro-ph.CO], 2013.

[25] D. Fixsen, The Temperature of the Cosmic Microwave Background, Astrophys.J., vol. 707, pp. 916-920, 2009, 0911.1955.

[26] Antonio Riotto, Inflation and the Theory of Cosmological Perturbations, arXiv:hep-ph/0210162.

[27] WMAP Collaboration (C.L. Bennett et al.), First year Wilkinson Microwave Anisotropy Probe (WMAP) observations: Preliminary maps and basic results, Astrophys.J.Suppl. 148 (2003) 1-27.

[28] Daniel Baumann, Cosmology: Part III Matehematical Tripos, http://www.damtp.cam.ac.uk/user/db275/Cosmology.pdf.

[29] Daniel Baumann, Physics of inflation, http://www.damtp.cam.ac.uk–/user/db275/TEACHING/INFLATION/Lectures.pdf.

[30] Edward W. Kolb and Michael S. Turner, 1990, The early Universe, Westview Press.

[31] A. R. Liddle and D. H. Lyth, False vacuum with Einstein Gravity, Phys. Rep. 231, 1 (1993).

[32] A. R. Liddle and D. H. Lyth, Cosmological Inflation and Large-Scale Structure, to be published by Cambridge University Press.

[33] C. Armendariz-Picon, T. Damour, and V. F. Mukhanov, k-inflation,Phys. Lett., B 458.

[34] Jaume Garriga, and V.F. Mukhanov, Perturbations in k-inflation, arXiv:hep-th/9904176v1 26 Apr 1999.

[35] Junko Ohashi and Shinji Tsujikawa, Observational constraints on assisted k-inflation, arXiv:1104.1565v1 [astro-ph.CO]

[36] Larissa Lorenz and Jerome Martin , K-inflationary Power Spectra in the Uniform Approximation, arXiv:0807.3037v2 [astro-ph]

[37] Larissa Lorenz and Jerome Martin, Constraints on Kinetically Modified Inflation from WMAP5, arXiv:0807.2414v1 [astro-ph]

[38] Ferdinand Helmer and Sergei Winitzki , Self-reproduction in k-inflation, arXiv:gr-qc/0608019v1.

[39] Kazuharu Bamba, Shinichi Nojiri, Sergei D. Odintsov and Diego Saez-Gomez, Inflationary universe from perfect fluid and F(R) gravity and its comparison with observational data, arXiv:1410.3993v2 [hep-th] .

[40] Qing-Guo Huang, A polynomial f(R) inflation model, arXiv:1309.3514v2 [hep-th].

[41] Taotao Qiu and Jun-Qing Xia, Perturbations of Single-field Inflation in Modified Gravity Theory, arXiv:1406.5902v2 [astro-ph.CO]

[42] Shinichi Nojiri and Sergei D. Odintsov, Dark energy, inflation and dark matter from modified F(R) gravity, arXiv:0807.0685v1 [hep-th].

[43] Antonio De Felice and Shinji Tsujikawa, $f(R)$ Theories, Living Rev. Relativity, 13, (2010), 3.

[44] Michal Artymowski and Zygmunt Lalak, Inflation and dark energy from $f(R)$ gravity, JCAP09(2014)036.

[45] Starobinsky, A. A., A New Type of Isotropic Cosmological Models Without Singularity. 1980, Phys.Lett., B91, 99.

[46] Ewan D. Stewart and David H. Lyth, A more accurate analytical calculation of the spectrum of cosmological perturbations produced during inflation, Phys. Lett B 302 (1993) 171-175.

[47] Daniel Baumann and Liam McAllister, Inflation and String Theory, arXiv:1404.2601v1 [hep-th].

[48] Stefan Antusch, David Nolde, BICEP2 implications for single-field slow-roll inflation revisited, JCAP 1405 (2014) 035.

[49] Daniel Baumann and Liam mcAllister, A Microscopic Limit on Gravitational Waves from D-brane Inflation, Phys. Rev. D 75, 123508 (2007).

[50] S Dimopoulos, S Kachru1, J McGreevy and J G Wacker, N-flation, JCAP08(2008)003 [hep-th/0507205].

[51] A. Ashoorioon, H. Firouzjahi and M.M. Sheikh-Jabbari, M-flation: Inflation From Matrix Valued Scalar Fields, JCAP 06 (2009) 018 [arXiv:0903.1481].

[52] A. Ashoorioon and M.M. Sheikh-Jabbari, Gauged M-flation, its UV sensitivity and Spectator Species, JCAP 06 (2011) 014 [arXiv:1101.0048].

[53] John McDonald, Sub-Planckian two-field inflation consistent with the Lyth bound, JCAP 1409 (2014) 09, 027.

[54] Tianjun Li, at. al, Helical Phase Inflation, Phys.Rev. D91 (2015) 061303.

[55] Tianjun Li, at. al, Helical Phase Inflation and Monodromy in Supergravity Theory, arXiv:1412.5093v1 [hep-th].

[56] Richard Easther, William H. Kinney, and Brian A. Powell, The Lyth Bound and the End of Inflation, JCAP 0608 (2006) 004.

[57] S. Kanemura, T. Matsui and T. Nabeshima, Higgs inflation in a radiative seesaw model, Phys. Lett. B 723 (2013) 126.

[58] E. Ma, Verifiable radiative seesaw mechanism of neutrino mass and dark matter, Phys. Rev. D 73, 077301 (2006).

[59] Nilendra G. Deshpande and Ernest Ma, Pattern of symmetry breaking with two Higgs doublets, Phys. Rev. D 18, 2574 (1978).

[60] Ethan M. Dolle and Shufang Su, Inert dark matter, Phys.Rev. D80 (2009) 055012 .

[61] M. Fukugita and T. Yanagida, Baryogenesis without grand unification, Phys. Lett. B174, 45 (1986).

[62] S. Weinberg, Baryon and Lepton Nonconserving processes, Phys. Rev. Lett. 43, 1566 (1979).

[63] V. A. Kuzmin, V. A. Rubakov, and M. E. Shaposhnikov, On anomalous elecroweak baryon-number non-conservation in the early universe, Phys. Lett. 155B, 36 (1985)

[64] Jisuke Kubo, Ernest Ma, Daijiro Suematsu, Cold Dark Matter, Radiative Neutrino Mass, mu to e gamma, and Neutrinoless Double Beta Decay, Phys.Lett. B642 (2006) 18-23.

[65] Shoichi Kashiwase and Daijiro Suematsu, Baryon number asymmetry and dark matter in the neutrino mass model with an inert doublet, Phys.Rev. D86 (2012) 053001.

[66] G.t Hooft and M. Veltman, Scalar one-loop integrals, Nucl. Phys. B153 (1979) 365-401.

[67] G. Passarino and M. Veltman, One-loop correction for e^+e^- annihilation into $\mu^+\mu^-$ in the Weinberg model, Nucl Phys B160 (1976) 151-207.

[68] Romain Bouchand, Radiative Neutrino Mass Generation and Renormalization Group Running in the Ma-Model, http://www.diva-portal.org/smash/get/diva2:517225/FULLTEXT01.pdf.

[69] Luis G. Cabral- Rosetti and Miguel A. Sanchis-Lozano, Appell Functions and the Scalar One-Loop Three-point Integrals in Feynman Diagrams, arXiv:hep-ph/0206081v2.

[70] Qing Gao and Yungui Gong, The challenge for single field inflation with BICEP2 result, Phys.Lett. B734 (2014) 41-43 [arXiv:1403.5716v2 [gr-qc] 17 May 2014].

[71] Tatsuo Kobayashi and Osamu Seto, Polynomial inflation models after BICEP2, Phys.Rev. D89 (2014) 103524 [arXiv:1403.5055 [astro-ph.CO]].

[72] P. A. R. Ade et al. [BICEP2 Collaboration], arXiv:1403.3985 [astro-ph.CO].

[73] D.H. Lyth, A. Riotto, Particle Physics Models of Inflation and Cosmological Density Perturbation, Phys. Rep. 314 (1999) 1.

[74] Armen Bagdasaryan, A Note on the 2F1 Hypergeometric Function, J. Math. Res. vol. 2, no. 3, (2010), 71-77, arXiv:0912.0917v1 [math.CA].

[75] Karen T. Kohl and Victor H. Moll, The integral in Gradshteyn and Ryzhik Part 20: Hyperbolic functions, SCIENTIA Series A: *Mathematical Sciences*, Vol. 21 (2011), 43-54.

[76] A. R. Liddle and D. H. Lyth, False vacuum with Einstein Gravity, Phys. Rep. 231, 1 (1993).

[77] A. R. Liddle and D. H. Lyth, Cosmological Inflation and Large-Scale Structure, to be published by Cambridge University Press.

[78] A.D. Linde, Chaotic inflation, Phys. Lett. B 129 (1983) 177.

[79] Xin Gao , Tianjun Li, and Pramod Shukla, Fractional-chaotic inflation in the lights of PLANCK and BICEP2, arXiv:1404.5230v5 [hep-ph].

[80] David H. Lyth, BICEP2, the curvature perturbation and supersymmetry, arXiv:1403.7323v4 [hep-ph].

[81] (P.A.R. Ade (Cardiff U.) et al, Planck 2015 results. XIII. Cosmological parameters, arXiv:1502.01589 [astro-ph.CO].

[82] M. Hazumi, Prog. Theor. Phys. Suppl. 190 (2011) 75.

[83] Lev Kofman, Andrei Linde and Alexei A. Starobinsky, Reheating after inflation, arXiv:hep-th/9405187v2.

[84] Lev Kofman, Andrei Linde and Alexei A. Starobinsky, Towards the Theory of Reheating After Inflation, arXiv:hep-ph/9704452v2.

[85] Rouzbeh Allahverdi, Robert Brandenberger, Francis-Yan Cyr-Racine and Anupam Mazumdar , Reheating in Inflationary Cosmology: Theory and Applications, arXiv:1001.2600 [hep-th].

[86] S. Kashiwase and D. Suematsu, Baryon number asymmetry and dark matter in the neutrino mass model with an inert doublet, Phys. Rev. D86 (2012) 053001.

[87] S. Kashiwase and D. Suematsu, Leptogenesis and dark matter detection in a TeV scale neutrino mass model with inverted mass hierarchy, Eur Phys. J C73 (2013) 2484.